



UNIVERSITY OF HELSINKI



<https://helda.helsinki.fi>

Helda

Climate Change, Summer Temperature, and Heat-Related Mortality in Finland : Multicohort Study with Projections for a Sustainable vs. Fossil-Fueled Future to 2050

Kivimäki, Mika

Public Health Services, US Dept of Health and Human Services

2023-12

Kivimäki, M, Batty, G D, Pentti, J, Suomi, J, Nyberg, S T, Merikanto, J, Nordling, K, Ervasti, J, Suominen, S B, Partanen, A-I, Stenholm, S, Käyhkö, J & Vahtera, J 2023, 'Climate Change, Summer Temperature, and Heat-Related Mortality in Finland : Multicohort Study with Projections for a Sustainable vs. Fossil-Fueled Future to 2050', Environmental Health Perspectives, vol. 131, no. 12, 127020. <https://doi.org/10.1289/EHP12080>

<http://hdl.handle.net/10138/593207>

10.1289/EHP12080

publishedVersion


Downloaded from Helda, University of Helsinki institutional repository.

This is an electronic reprint of the original article.

This reprint may differ from the original in pagination and typographic detail.

Please cite the original version.

Climate Change, Summer Temperature, and Heat-Related Mortality in Finland: Multicohort Study with Projections for a Sustainable vs. Fossil-Fueled Future to 2050

Mika Kivimäki,^{1,2,3} G. David Batty,¹ Jaana Pentti,^{2,3,4,5} Juuso Suomi,⁶ Solja T. Nyberg,^{2,3} Joonas Merikanto,⁷ Kalle Nordling,^{7,8} Jenni Ervasti,³ Sakari B. Suominen,^{4,9,10} Antti-Ilari Partanen,⁷ Sari Stenholm,^{4,5} Jukka Käyhkö,⁶ and Jussi Vahtera^{4,5,9} 

¹University College London (UCL) Brain Sciences, UCL, London, UK

²Clinicum, Faculty of Medicine, University of Helsinki, Helsinki, Finland

³Finnish Institute of Occupational Health, Helsinki, Finland

⁴Department of Public Health, University of Turku (UTU), Turku, Finland

⁵Centre for Population Health Research, UTU, Turku, Finland

⁶Department of Geography and Geology, UTU, Turku, Finland

⁷Finnish Meteorological Institute, Helsinki, Finland

⁸Centre for International Climate and Environmental Research, Oslo, Norway

⁹Turku University Hospital, Turku, Finland

¹⁰School of Health Science, University of Skövde, Skövde, Sweden

BACKGROUND: Climate change scenarios illustrate various pathways in terms of global warming ranging from “sustainable development” (Shared Socioeconomic Pathway SSP1-1.9), the best-case scenario, to “fossil-fueled development” (SSP5-8.5), the worst-case scenario.

OBJECTIVES: We examined the extent to which increase in daily average urban summer temperature is associated with future cause-specific mortality and projected heat-related mortality burden for the current warming trend and these two scenarios.

METHODS: We did an observational cohort study of 363,754 participants living in six cities in Finland. Using residential addresses, participants were linked to daily temperature records and electronic death records from national registries during summers (1 May to 30 September) 2000 to 2018. For each day of observation, heat index (average daily air temperature weighted by humidity) for the preceding 7 d was calculated for participants’ residential area using a geographic grid at a spatial resolution of 1 km × 1 km. We examined associations of the summer heat index with risk of death by cause for all participants adjusting for a wide range of individual-level covariates and in subsidiary analyses using case-crossover design, computed the related period population attributable fraction (PAF), and projected change in PAF from summers 2000–2018 compared with those in 2030–2050.

RESULTS: During a cohort total exposure period of 582,111,979 summer days (3,880,746 person-summers), we recorded 4,094 deaths, including 949 from cardiovascular disease. The multivariable-adjusted rate ratio (RR) for high ($\geq 21^\circ\text{C}$) vs. reference ($14\text{--}15^\circ\text{C}$) heat index was 1.70 (95% CI: 1.28, 2.27) for cardiovascular mortality, but it did not reach statistical significance for noncardiovascular deaths, RR = 1.14 (95% CI: 0.96, 1.36), a finding replicated in case-crossover analysis. According to projections for 2030–2050, PAF of summertime cardiovascular mortality attributable to high heat will be 4.4% (1.8%–7.3%) under the sustainable development scenario, but 7.6% (3.2%–12.3%) under the fossil-fueled development scenario. In the six cities, the estimated annual number of summertime heat-related cardiovascular deaths under the two scenarios will be 174 and 298 for a total population of 1,759,468 people.

DISCUSSION: The increase in average urban summer temperature will raise heat-related cardiovascular mortality burden. The estimated magnitude of this burden is > 1.5 times greater if future climate change is driven by fossil fuels rather than sustainable development. <https://doi.org/10.1289/EHP12080>

Introduction

Global warming is a major public health challenge.^{1–3} Vulnerable people, particularly the old and infirm, are likely to be most affected. By increasing cardiovascular strain (predisposing to ischemia) and inflammatory responses (elevating the risk of thrombosis), heat is known to be associated with excess mortality from ischemic heart disease, stroke, and heart failure.^{4–12} Studies have also found elevated risk of other causes of death, including respiratory diseases, infectious and digestive system diseases, and some external causes, such as suicide.^{3,13,14} The extent to which global warming will affect future summertime heat-related mortality is, however, uncertain and is likely to be dependent on the characteristics of climate change.

Shared Socioeconomic Pathways, or SSPs, are widely used to characterize how societal, demographic, and economic change might modify the course of global warming over the next decades. The most pernicious SSP option, the “fossil-fueled development—no mitigation” scenario [Coupled Model Intercomparison Project Phase 6 (CMIP6) SSP5-8.5]¹⁵ posits that rapid economic and social development coupled with continued resource- and energy-intensive lifestyles and exploitation of abundant fossil fuel resources will produce an accelerated unfavorable shift in global weather patterns.¹⁶ By contrast, the most positive development scenario, “taking the green road—very ambitious mitigation” (SSP1-1.9), forecasts success in efforts toward lower material growth, lower resource and energy intensity, and developments that respect perceived environmental boundaries, in doing so, reducing the pace of global warming.¹⁶ Recent reviews of studies estimating future mortality suggest that deaths from high temperatures will increase with global warming across different scenarios,^{12,17,18} although estimates rarely include future changes in population demographics. Furthermore, the projections have typically been based on crude aggregate-level data rather than cohort studies that enable control for individual-level covariates, such as demographic characteristics (age, sex, and socioeconomic position), residential area characteristics (e.g., neighborhood deprivation) and lifestyle factors (obesity, alcohol consumption), or study designs with strong internal validity, such as the case-crossover approach.^{18–27}

Accordingly, in this study, we used individual-level daily spatiotemporal data to make projections regarding future heat-related mortality burden. Specifically, we aimed to, first, examine the

Address correspondence to Jussi Vahtera, Department of Public Health, University of Turku, Kiinamyllynkatu 10, 20520 Turku, Finland. Email: jussi.vahtera@utu.fi

Supplemental Material is available online (<https://doi.org/10.1289/EHP12080>).

The authors declare they have nothing to disclose.

Received 30 August 2022; Revised 16 November 2023; Accepted 17 November 2023; Published 27 December 2023; Corrected 26 March 2024.

Note to readers with disabilities: *EHP* strives to ensure that all journal content is accessible to all readers. However, some figures and Supplemental Material published in *EHP* articles may not conform to 508 standards due to the complexity of the information being presented. If you need assistance accessing journal content, please contact ehpsubmissions@niehs.nih.gov. Our staff will work with you to assess and meet your accessibility needs within 3 working days.

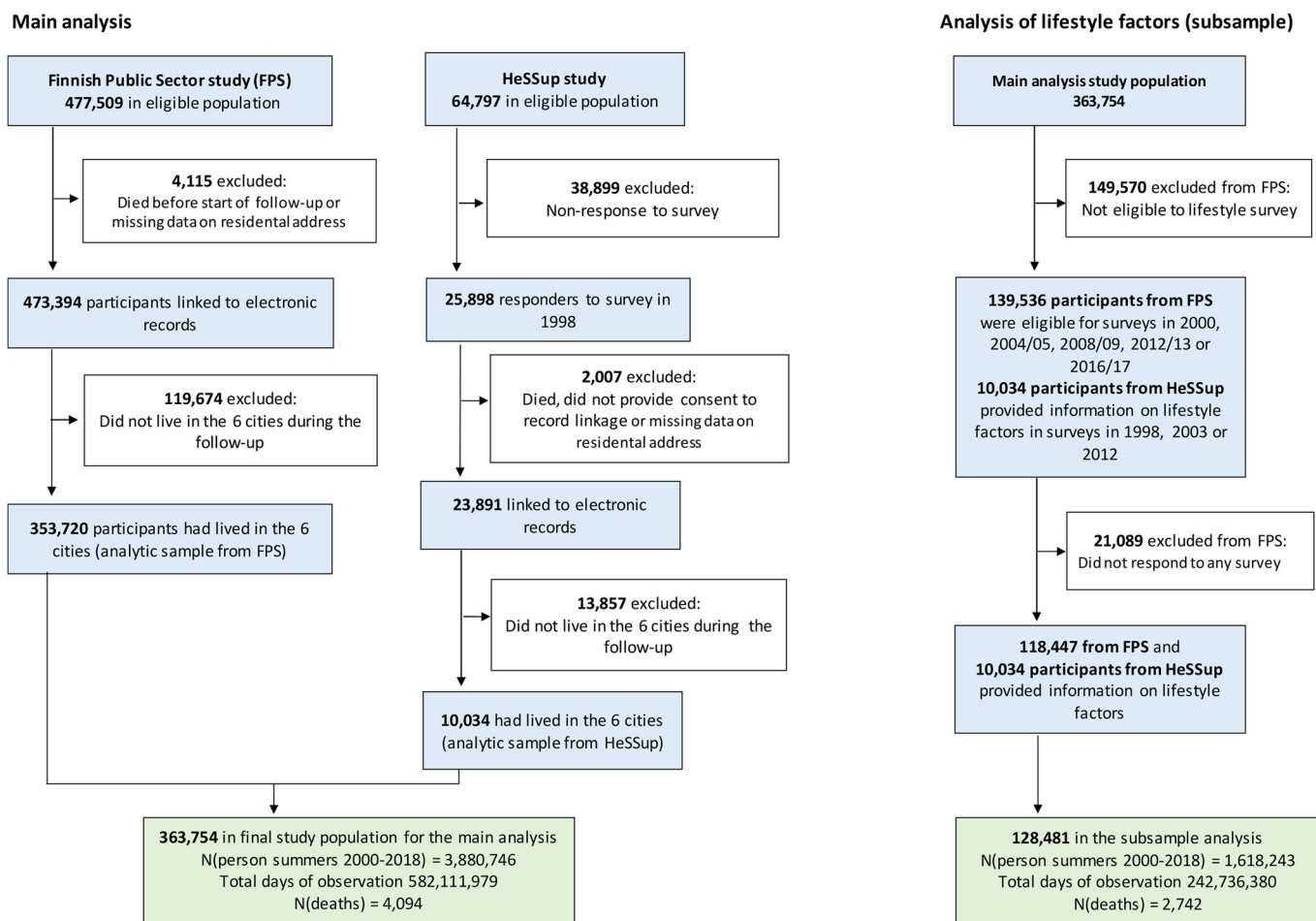


Figure 1. Selection of participants living in six Finnish cities from two cohort studies, 2000–2018. Summertime is between and 1 May and 30 September, a total of 150 d. Note: HeSSup, Health and Social Support Study.

association of summer temperature with cause-specific deaths in the general population and then by subgroups of age, sex, education, and characteristics of residential building and neighborhoods and lifestyle profile. Second, we tested whether these associations were biased by using a case-crossover design in which each individual served as their own control.²⁸ Third, by using these estimates, the observed trends in temperature from 1980 to 2019, and projected demographic changes in population demographics, we estimated heat-related mortality burden in future summers (2030–2050) separately for the fossil-fueled development and sustainable development scenarios.¹⁶ Our analyses of mortality burden are for the six largest cities in Finland, a country where summers are mild, but projected future increases in temperature are, in fact, more rapid than in those at lower latitudes.²⁹

Methods

Study Context

In Finland, the yearly average temperature has risen almost 2°C since the beginning of the 20th century to the present, double the rate of the global average.^{30,31} During 1961–2019, all months besides June have shown a warming trend, the annually averaged warming over this period being 2.10°C in Southern Finland (60 to <64°N) and 2.25°C in the North (64–68°N). The absence of warming in June has been ascribed to persistent changes in atmospheric circulation patterns during that month.³²

Data

We used pooled data from participants in two well-characterized Finnish prospective cohort studies, the Health and Social Support Study (HeSSup)³³ and the Finnish Public Sector study (FPS).³⁴ These studies include people residing in Finland’s six largest cities, based on the number of inhabitants (Helsinki, Espoo, Tampere, Vantaa, Oulu, and Turku). The selection of the analytical sample is shown in Figure 1. The FPS is an occupational cohort comprising 353,720 men and women who, as of 1990–2016, worked in the public sector, lived in the target cities, had longitudinal data on residential locations (with dates of moves) and socioeconomic characteristics, and were successfully linked to death records from the national mortality register until 31 December 2018. In the analysis of lifestyle factors, we used a subsample of 118,447 participants who responded to one or more of the five lifestyle surveys conducted between 1 September 2000 and 1 September 2017 (response to at least one survey: 84.9%).

In the population-based HeSSup study, as of 1998, 10,034 men and women lived in the target cities, responded to a questionnaire survey on socioeconomic characteristics and lifestyle factors between 1 June 1998 and 31 May 2000, 1 January and 31 August 2003, and 1 December 2011 and 31 August 2012, had longitudinal data on residential locations, and were successfully linked to death records from the national mortality register until 31 December 2015.

The total analytic sample included 363,754 participants from the two cohort studies. Analyses of lifestyle factors were based on a subsample of 128,481 participants, including a subsample from

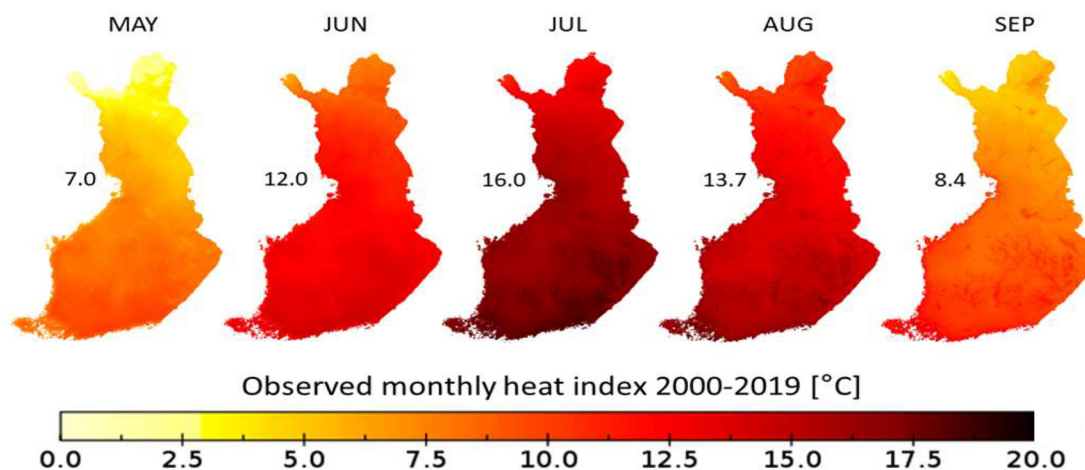


Figure 2. Spatial distribution of monthly heat index (1 km × 1 km resolution) in Finland, averaged over 2000–2019. The number to the left of each heat map is the countrywide monthly average heat index (°C). The corresponding monthly average temperature is slightly higher than the monthly average heat index: 8.2°C (May), 12.9°C (June), 16.4°C (July), 14.1°C (August), and 9.2°C (September). Note: AUG, August; JUL, July; JUN, June; SEP, September.

the FPS ($N = 118,447$) and the total sample from the HeSSup ($N = 10,034$). The FPS was approved by the ethics committee of the Hospital District of Helsinki and Uusimaa (HUS/1210/2016) and the HeSSup, by the ethics committee of Turku University Hospital and the Finnish Population Register Centre (VRK 2605/410/14).

Measures

We used observational daily mean weather data interpolated over Finland to a spatial resolution of 1 km × 1 km.³⁵ The data were obtained from the Finnish Meteorological Institute and were based on the Kriging interpolation accompanied by external predictors (e.g., topography and water bodies) of continuous observational records from >500 weather stations in Finland, supplemented with continuous station data from neighboring countries.³⁵ In the present analyses we used continuous daily gridded time series of daily mean temperature and relative humidity for May–September 1980–2019. These are the five warmest months in Finland. The original data set has been cross-validated; the correlation coefficient R^2 was 0.99 for daily mean temperature and 0.88 for relative humidity. In summer months, the root-mean-square error was lowest for daily mean temperature (0.58°C in July) and highest for relative humidity (5.9% in July).³⁵

We obtained geocoded residential addresses for participants from the Population Register Centre of Finland. Participants' residential locations were linked to information on ambient temperature using a geographic grid at a spatial resolution of 1 km × 1 km between 1 May and 30 September for each of the years 2000 to 2019. These data were updated on a daily basis.

Summertime heat index. Different indicators of heat exposure are strongly correlated and cross-validation studies suggest there is no single optimal temperature measure for mortality research.^{36–38} Our main exposure was summertime heat index as defined by the U.S. National Oceanic and Atmospheric Administration (NOAA), a measure that has been used in other heat exposure–mortality studies across diverse environments.^{39–41} A heat index value for each day was calculated based on daily mean temperature and humidity values using the following equation:

$$HI_F = 0.5 \times \{T + 61.0 + [(T - 68.0) \times 1.2] + (RH \times 0.094)\},$$

where T is the temperature (in degrees Fahrenheit), and RH is the relative humidity.⁴² This index was converted to degrees Celsius

using the following formula: $HI_C = (HI_F - 32) \times 5/9$. Figure 2 shows the 2000–2019 monthly average heat index in Finland for each month from May to September from 2000–2019.

For each day of observation, we calculated the average 7-d heat index, including the same day and the previous 6 days. Definitions of “high heat” vary between studies, with common distribution-based thresholds ranging between the 95th, 97.5th, and 99th percentiles.^{36,43,44} To allow sufficient case numbers in statistical analyses, we used the 95th percentile (representing a heat index of 21°C) during summers in 2000–2018 as the threshold for the high heat index. After rounding the values to the nearest integer, we categorized the heat index into six categories: 13°C or less, 14–15°C, 16–17°C, 18–19°C, 20°C, and ≥21°C, the reference being 14–15°C, the temperature with minimum mortality in Finland.⁴⁵

Alternative measures of heat exposure. To examine the robustness of our findings, we conducted subsidiary analyses using three alternative heat measures: *a*) lag 0–1 using a mean heat index of the same and previous day (i.e., 2-d heat index), *b*) a 7-d mean of daily maximum temperatures (i.e., 7-d Tmax), and *c*) a 2-d mean of daily maximum temperatures (i.e., 2-d Tmax). The 95th percentile defining the threshold for high heat was 21°C for the 2-d heat index and 26°C for the two maximum temperature indices.

Characteristics of residential location. To examine area-level indicators that may modify the association between heat and mortality, we conducted stratified analyses by characteristics of residential location. These included four participant-level variables: *a*) the type of building in which the participant resided, *b*) neighborhood greenness, *c*) area deprivation, and *d*) living in an urban heat island. These variables were dichotomized to enable sufficient case numbers in our analyses. We obtained data on building type (single-family home vs. not) from the Population Register Centre of Finland for each residential address, and this information was updated daily during follow-up. To assess the degree of residential surrounding green space, we linked participants' addresses to the mean Normalized Difference Vegetation Index (NDVI) calculated for each 250 m × 250 m grid area from a satellite image composite using Google Earth Engine, as described previously.^{46,47} For subgroup analyses, we dichotomized this variable into high (NDVI > 0.45) vs. low (≤ 0.45) surrounding green space. Participants' residential addresses were linked to data on neighborhood deprivation obtained from Statistics Finland. The deprivation index is based on the proportion of adults with low education, the unemployment rate, and household mean income in each

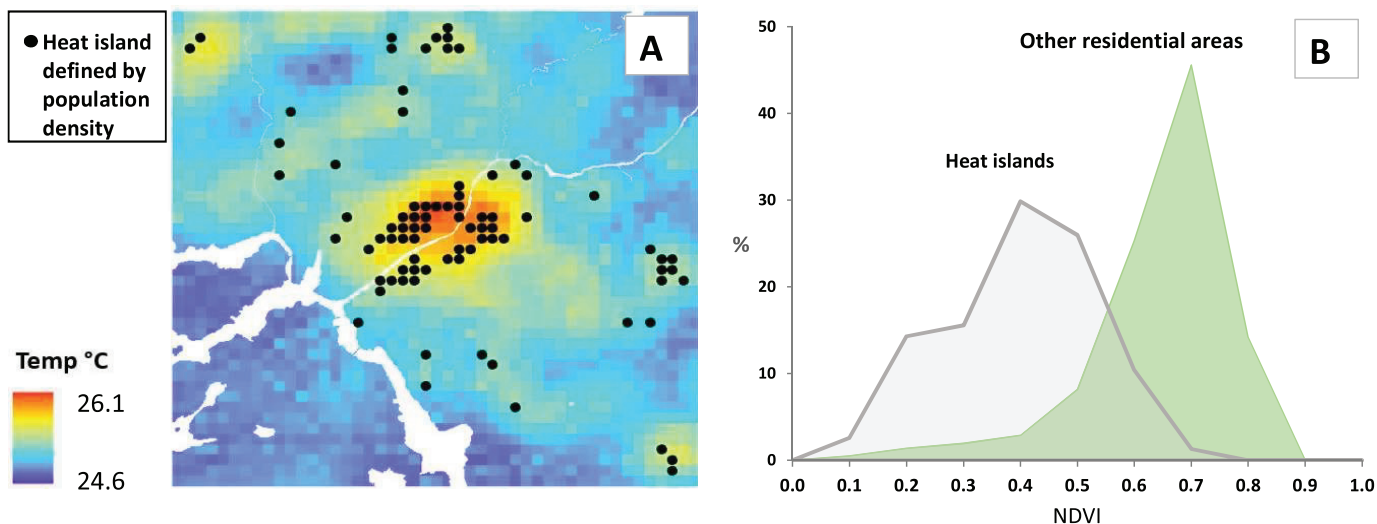


Figure 3. Validation of the density-based definition of heat island using additional high-resolution temperature and NDVI measurements. (A) Data from a 12 km × 12 km area of the city Turku, June 2018. Urban heat islands, defined by a population density of ≥ 500 people per 250 m × 250 m grid, are shown by black circles. Colors ranging from blue to red indicate temperatures in these grids. (B) The distribution of NDVI by urban heat island status in the same area and at the same time period. The mean ± SD of the NDVI was lower in urban heat islands (0.40 ± 0.14) than elsewhere (0.65 ± 0.12, *t*-test, *p* < 0.0001). Note: AUG, August; JUL, July; JUN, June; NDVI, Normalized Difference Vegetation Index; SD, standard deviation; SEP, September.

250 m × 250 m grid area⁴⁶ and was categorized into low (area deprivation value < national mean) vs. high neighborhood deprivation (deprivation value > national mean). NDVI and neighborhood deprivation were updated based on moving during follow-up.

Because the interpolation of the heat index data did not account for urban surfaces or heating, we constructed a proxy for regions with potential urban heat island effects using information on population density from Statistics Finland. Participants were considered to be living in regions with an urban heat island effect if they were resident in a densely populated area (population density ≥ 500 per 250 m × 250 m grid area). These data are updated annually. We validated our heat island proxy measure by using high-resolution measurement of mean temperatures for a 7-d period in June 2018 as measured in Turku, one of the cities featured in our study. Linear regression model using geographical information system data on land use, topography, and water bodies as independent variables, using temperature observations of a local network of 71 HOBO U23 Pro v2 temperature and relative humidity data loggers in the Turku area [Turku Urban Climate Research Group (TURCLIM); <https://sites.utu.fi/turclim/>]. In Figure 3A, heat islands defined by population density are shown by black circles, and colors ranging from blue to red indicate temperatures in the 250 m × 250 m grid. Regions with urban heat island effects based on population density corresponded well with the hottest regions based on high-resolution temperature measurement (the TURCLIM heat map).

Given that impervious surfaces are a key contributor of the urban heat island effect, we examined differences in NDVI distributions between heat islands defined by population density and other locations (low NDVI is related to impervious surfaces). Supporting the validity of our proxy measure, the mean ± SD of the NDVI was significantly lower in urban heat islands (0.40 ± 0.14) than elsewhere (0.65 ± 0.12, *t*-test, *p* < 0.0001; Figure 3B).

Demographic and lifestyle-related covariates. To examine individual-level indicators that may modify the association between heat and mortality, we conducted analyses stratified by age (< 65 vs. ≥ 65 y), sex, education (primary vs. secondary or higher), and lifestyle factors. Data on age and sex were obtained from employers' registers (for the FPS) or Statistics Finland (for the HeSSup) and education from Statistics Finland (for the FPS) or questionnaire

survey (for the HeSSup). In both cohorts, we assessed four lifestyle-related risk factors using standard survey instruments and categorized using standard thresholds⁴⁸: *a*) obesity (body mass index ≥ 30 kg/m² vs. lower), *b*) current or former smoker (vs. never smoker), *c*) high alcohol intake (> 14 units of alcohol per week or binge drinking vs. other), and *d*) physical inactivity [metabolic equivalent of task (MET)-hours < 14 and other]. We also constructed a lifestyle index as the sum of lifestyle risk factors (range 0–4; with a lower score denoting healthier levels). For subgroup analysis, this variable was dichotomized into healthy (0–1 of obesity, smoking, high alcohol intake, physical inactivity) vs. unhealthy lifestyle (2–4 of these four risk factors).

Mortality ascertainment. By using their unique national identification number, participants were linked to the national register of mortality kept by Statistics Finland. The records included date and primary cause of death coded according to the World Health Organization's *International Classification of Diseases, Tenth Revision*⁴⁹ (ICD-10). We identified the most common causes of mortality: from cancer (ICD-10 codes C00–C97), cardiovascular diseases (ICD-10 codes I00–I99), external causes (ICD-10 codes V01–Y86), and other causes (all other ICD-10 codes). Total (all-cause) mortality was also used as an outcome in its own right.

Future Climate Change Scenarios

The climate science community has designed sets of scenarios that span an array of possible futures for climate policy, global economy, land use, emissions, resulting greenhouse gas concentrations, and climate change.¹⁶ For this study, we chose two extreme scenarios: *a*) SSP1-1.9, which is the most stringent emission reduction scenario based on the sustainable development with a radiative forcing of 1.9 W/m² at 2,100⁵⁰; and *b*) SSP5-8.5, which is based on the fossil-fueled development with a radiative forcing of 8.5 W/m² at 2,100.⁵¹ Hereafter, these are simply referred as “sustainable development” and “fossil-fueled development” scenarios, respectively. The CMIP6 data were downloaded from the Earth System Grid Federation (ESGF) data archive (<https://esgf-data.dkrz.de/search/cmip6-dkrz/>) accessed through Google Cloud (<https://console.cloud.google.com/marketplace/product/noaa-public/cmip6>). We used estimates of

change in future temperature and heat index that were averaged and weighted across the following eight climate change models available for both the sustainable development scenario and the fossil-fueled development scenario: GFDL-ESM4,^{52–55} IPSL-CM6A-LR,^{56–59} MIROC6,^{60–63} MRI-ESM2-0,^{64–67} CanESM5,^{68–71} CAMS-CSM1-0,^{72–75} FGOALS-g3,^{76–79} and EC-Earth3-Veg.^{80–83}

Statistical Analysis

To determine the association between summertime heat and mortality, we used four different analytic approaches. First, we examined the associations of 7-d average heat exposure with all-cause and cause-specific mortality. Using Poisson regression analyses adjusted for age, sex, and calendar year, we calculated the number of deaths per 10,000 during summer periods for each exposure category and the corresponding mortality rate ratios (RRs) and their 95% confidence intervals (CIs) for heat index categories $\leq 13^\circ\text{C}$, $16\text{--}17^\circ\text{C}$, $18\text{--}19^\circ\text{C}$, 20°C , and $\geq 21^\circ\text{C}$ compared with the reference category (heat index $14\text{--}15^\circ\text{C}$). Multivariable-adjusted analyses were controlled for age, sex, calendar year and additionally for demographic (education), residential (type of building, greenness, neighborhood deprivation, population density), and lifestyle-related (obesity, smoking, high alcohol intake, physical inactivity) covariates. To examine whether the heat-related risk of death varied depending on sex, age, education, building type, NDVI, neighborhood deprivation, urban heat island status, obesity, smoking, alcohol consumption, and physical inactivity, we stratified analyses by these factors and reported strata-specific effect estimates. Interactions between summertime heat and covariates were tested by computing an interaction term, heat index \times covariate. In these analyses, covariates were dichotomized to maintain statistical power.

To examine the burden of heat-related mortality during summers, we calculated periodic population attributable fractions (PAFs) with bootstrap 95% CIs using the following formulas:

$$PAF \text{ in group } j = P_j(RR_j - 1) / \left[1 + \sum_{i=1}^K P_i(RR_i - 1) \right],$$

$$PAF = \sum_{j=1}^K PAF_j,$$

where P_i is the proportion of the population in group i ; RR_i is the RR in group i ; and K is the number of non-reference risk groups.

Second, we evaluated the robustness of the heat–mortality association by using a case-crossover design. This method effectively controls for all measured and unmeasured time-invariant confounders because only the cases are included.⁸⁴ We used conditional logistic regression and bidirectional control sampling design to examine whether the odds of exposure to high heat index ($\geq 21^\circ\text{C}$ vs. $\leq 20^\circ\text{C}$) was higher in the case time (the 7-d period within which the person died) compared with the odds in the control times (the corresponding 7-d period 1 y earlier and 1 y later). To further examine the robustness of the findings, this analysis was repeated using control dates that were the same day of the weeks as the day of death (e.g., Monday) during the case month. In both analyses, the results were expressed as odds ratios (ORs) with accompanying 95% CIs. In secondary analyses, we repeated steps 1 and 2 after replacing heat index with alternative indicators: lag 0–1 using mean heat index of the same and previous day (2-d heat index); 7-d mean of daily maximum temperatures; and 2-d mean of daily maximum temperatures. In the first indicator, high heat referred to $\geq 21^\circ\text{C}$ and the reference, to $14\text{--}20^\circ\text{C}$. The corresponding categories for the latter two indicators were to $\geq 26^\circ\text{C}$ for high and $19\text{--}25^\circ\text{C}$ for the reference.

Third, for the future projections of the heat index, we used a 40-y time series of observational data as a basis. The monthly averaged heat index during 1980–1999 and 2000–2019 was calculated for each grid cell from observational data. The difference in the average monthly heat index maps between the two time periods, divided by two decades, represents the decadal change in monthly average heat index in each location. In the current warming trend scenario, we assume that the observed (1980–1999 to 2000–2019) average monthly rate of change in heat index remains unchanged until 2050. This allowed us to generate a projection of the future heat index time series for each $1 \text{ km} \times 1 \text{ km}$ grid cell by adding the observed decadal change in monthly location-specific heat index to the daily observed heat index values in the 2000–2019 observational data for that same month. We assumed that the spatially resolved heat index pattern relative to mean temperature is constant. This assumption is based on studies suggesting that spatial temperature change pattern relative to global mean temperature change (or cumulative carbon dioxide emissions) remains stable,⁸⁵ applies to seasonal temperatures⁸⁶ and temperature extremes,⁸⁷ and can be scaled for extreme heat.⁸⁸ We also anticipated that adaptation to heat remains unchanged until 2050.

We predicted heat index and corresponding PAFs and their 95% CIs in heat-related excess mortality during summer periods in 2030–2050 using *a*) observations on the heat–mortality associations at the population level from 2000 to 2018, and *b*) the observed monthly spatially resolved change in heat index between two 20-y summer periods (2000–2019 vs. 1980–1999). In the current warming trend scenario, we assumed the observed risk ratios (RRs) would remain unchanged for the near future.²⁴ We estimated PAFs for future heat-related excess mortality for summer periods in 2030–2050 based on the current warming trend scenario and two other climate change scenarios. We calculated the future heat index for the sustainable (SSP1-1.19) and fossil-fueled (SSP5-8.5) development scenarios in Finland, scaling the current warming trend heat index projections by the ratio of average May–September warming trend between the SSP and historical simulations in the CMIP6 ensemble (i.e., SSP1-1.19/historical and SSP5-8.5/historical). The historical data were available until 2014 and extended based on SSP5-8.5 for the years 2015–2019. Scaling observed trends based on climate model data reduces regional biases because climate models are used to project only relative trends. The rationale for this method is the same as that for the current warming trend scenario.

To reduce the “hot model” bias (i.e., error caused in estimation by giving too much weight for models that project more warming than assessment of multiple other lines of evidence suggests),^{89,90} we weighted each model depending on how close its transient climate response (TCR) is to the best estimate of 1.8°C in the Intergovernmental Panel on Climate Change, Assessment Report 6 (IPCC AR6).⁹¹ Weights were calculated for each model by evaluating a normal distribution density function fitted to match the very likely 90% range of TCR ($1.2\text{--}2.4^\circ\text{C}$) at the TCR value of each model. We then used the weighted mean of heat index trends from the eight climate models as our best estimate for the two SSP scenarios and calculated the 95% credible interval (CrI) based on a fitted probability density function using kernel density estimation.

Fourth, taking into account demographic changes, we estimated summertime heat-related cardiovascular death burden in all citizens of the six cities under investigation by climate change scenario. We obtained demographic characteristics and the numbers of deaths for each city at the midpoint of the observation period 2000–2018 (2010) and projections of demographic characteristics and deaths at midpoint of 2030 and 2050 (2040) from Statistics Finland.^{92–94} For the period 2000–2018, we estimated

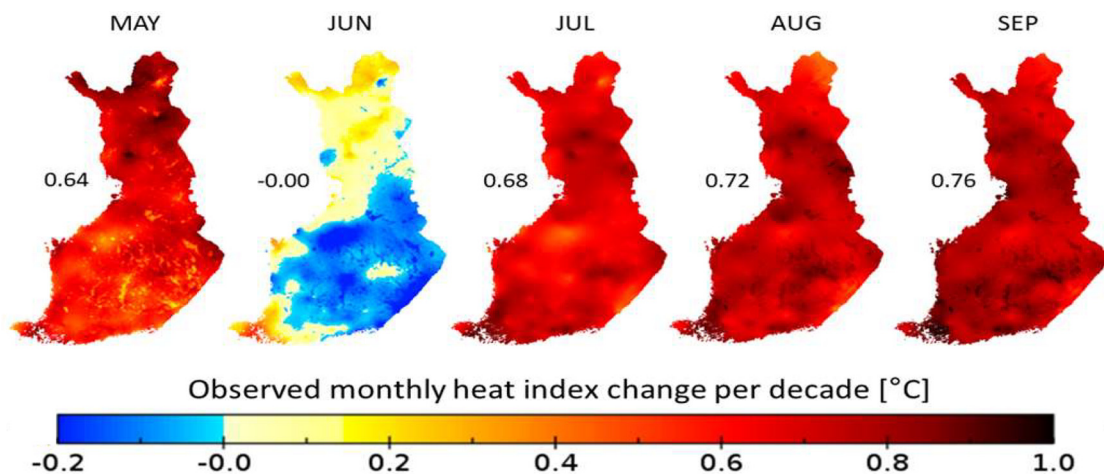


Figure 4. Spatial distribution of decadal May–September heat index change in Finland between 1980–1999 and 2000–2019. The number to the left of each heat map is the countrywide average decadal change in heat index between 1980–1999 and 2000–2019. The corresponding average decadal change in monthly temperature is: 0.57°C (May), –0.02°C (June), 0.58°C (July), 0.63°C (August), and 0.66°C (September).

weighted RRs of mortality for high heat index based on age- and sex-specific RRs (four groups: men <65 and ≥65 years of age and women <65 and ≥65 years of age) and the age and sex distribution in the six cities in 2010. For the period 2030–2050, we used the same age- and sex-specific RRs with predicted age and sex distribution in these cities in 2040. We computed weighted PAF for the observation period (2000–2018) and future climate change scenarios (2030–2050) using these effect estimates and the numbers of people in each population subgroup. For comparison, we computed weighted PAF for temperature changes of 0°C and 1°C per decade; these approximately represent the lower and upper ends of the 95% CrIs of the climate change scenarios. The corresponding heat index trends were 0°C and 1.152°C per decade, respectively.

Warming trend analyses were conducted using Python 3 and all mortality analyses were performed using SAS statistical software (version 9.4; SAS Institute, Inc.). Statistical significance was inferred at a two-tailed $p < 0.05$. Statistical code for the analysis and data sharing statement are provided in the “Statistical Code” section of the Supplemental Material in “Analysis of raw cmip6 warming trends,” “Analysis of weighted cmip6 warming trends,” and “Analysis of heat – mortality associations.” All respondents of the two cohort studies gave informed consent.

Results

Observed Climate Change in Finland

Figure 4 shows that the observed rate of change in the heat index is relatively uniform in Finland. However, the warming over large lakes is less pronounced during early summer and more pronounced during late summer, compared with that over land areas, and the increasing trend in heat index over time is stronger in coastal compared with inland regions. The spatial correlation coefficient calculated for the 1980–2019 May–September period using either odd- or even-numbered years only is 0.51 (with corresponding values of 0.77 for relative humidity change and 0.53 for temperature change). This supports the assumption that the future projections based on observed trends in spatial distribution of heat index from 1980–1999 to 2000–2019 will persist. Figure 4 also shows that, unlike in other months, there is little warming in June, an anomaly that has persisted over the 59 y of observations.³⁰

Overall, the temperature and humidity trends for the summer periods 1980–1999 and 2000–2019 were robust. For example, the mean decadal changes in temperature and humidity in Finland (decadal temperature change, 0.49°C; decadal relative humidity change, 1.05%) closely resembled those derived from the time series spanning even-numbered years (decadal temperature change, 0.51°C; decadal relative humidity change, 0.95%) or only odd years (decadal temperature change, 0.46°C; decadal relative humidity change, 1.16%).

Projected Climate Change in Finland

The observed summertime (May–September) warming trend in Finland from 1980–1999 to 2000–2019 was 0.486°C per decade. The corresponding relative humidity increase was 1.05% per decade, and the heat index change was 0.560°C per decade. This heat index trend was used for the current warming trend scenario for the years 2020 to 2050. Table 1 shows warming trends in CMIP6 models for the future period of 2020–2050 by SSP climate scenario. The weighted mean warming trends in the sustainable development and the fossil-fueled development scenarios between 2020 and 2050 were 0.225°C per decade and 0.528°C per decade, respectively. The corresponding increases in heat index were 0.259°C and 0.608°C per decade.

Association between Heat and Mortality

The cohort with valid data for analyses of heat index and cause-specific mortality comprised 363,754 men and women, with a mean ± SD age of 35.3 ± 12.8 y at baseline and 45.7 ± 15.4 y at the end of the mean follow-up of 10.7 person-summers (Table 2). The average cumulative 7-d heat index was 14.0°C. During 582,111,979 summer days at risk, we recorded a total of 4,094 deaths. Of the deaths, 1,574 were from cancer, 949 from cardiovascular disease, 694 from external causes, and 877 from other causes. The mean ± SD of the age at death was 60.1 ± 12.9 y.

Table 3 shows the association of heat index with all-cause and cause-specific mortality. After adjustment for age, sex, and calendar year, the mortality rate was 10.5 (95% CI: 9.8, 11.3) per 10,000 summers for heat index of 14–15°C (the reference category) and 13.3 (95% CI: 11.7, 15.1) per 10,000 summers for high heat index (21°C or higher). In relative terms, the calendar year-adjusted mortality RR was 1.27 (95% CI: 1.10, 1.46) times higher for those with a high heat index than for the reference group. The

Table 1. Change in temperature (°C) and heat index (°C) per decade in Finland based on scaling the observed trend with the ratio of warming trends between SSP and historical simulations in the Coupled Model Intercomparison Project, phase 6.

	Warming trend ^a		Weight ^b
	SSP1-1.9	SSP5-8.5	
Climate model, change in temperature			
GFDL-ESM4	-0.11	0.20	0.19
IPSL-CM6A-LR	0.61	1.15	0.07
MIROC6	0.41	0.93	0.17
MRI-ESM2-0	0.14	0.46	0.20
CanESM5	0.47	0.76	0.01
CAMS-CSM1-0	0.28	0.25	0.21
FGOALS-g3	0.32	0.68	0.15
EC-Earth3-Veg	-0.02	0.38	0.01
Weighted mean change in			
Temperature per decade (95% CrI)	0.22 (-0.29, 0.71)	0.53 (-0.14, 1.32)	—
Heat index per decade (95% CrI)	0.26 (-0.34, 0.82)	0.61 (-0.16, 1.52)	—

Note: The upper part of the table shows warming trends based on individual models and weights estimated for each model. The lower part shows weighted means and 95% CrIs for warming and heat index trends. —, Not applicable; CMIP6, Coupled Model Intercomparison Project, phase 6; CrI, credible interval; IPCC AR6, Intergovernmental Panel on Climate Change, Assessment Report 6; SSP1-1.9, Shared Socioeconomic Pathway (sustainable scenario); SSP5-8.5 (fossil-fueled scenario); TCR, transient climate response.

^aNumbers are projected changes in temperature in Celsius degrees per decade between 2020 and 2050 unless otherwise stated.

^bWeights obtained by comparing each model's TCR to the very likely range of IPCC AR6 were used to reduce hot model bias in estimates of mean change in temperature and heat index per decade and 95% CrIs.

corresponding RR was 1.71-fold (95% CI: 1.29, 2.26) for cardiovascular deaths, but it did not reach statistical significance for deaths from cancer or external causes or for mortality from other causes (causes of death other than cancer, cardiovascular disease, or external causes). The association between higher heat index and higher rate of cardiovascular deaths remained statistically significant after adjustments for age, sex, calendar year, education, type of building, greenness, neighborhood deprivation, population density, obesity, smoking, high alcohol intake, and physical inactivity (Table 4). For all noncardiovascular causes combined, we did not observe higher rates of death.

The main results were replicated in case-crossover analyses, suggesting that the associations between heat index, total mortality, and cardiovascular mortality were not related to confounding by stable differences between exposure groups or choice of control time (Figure 5). A high vs. lower heat index was associated with a 1.31-fold (95% CI: 1.11, 1.54) higher odds of mortality from all-causes and 1.98-fold (95% CI: 1.41, 2.78) higher odds of death from cardiovascular disease compared with control dates 1 y before and after the date of death. The corresponding ORs were slightly lower [OR = 1.21 (95% CI: 1.03, 1.44) and 1.46 (95% CI: 1.06, 2.00)], but statistically significant when this analysis was repeated using control dates that were the same day of the weeks as the day of death (e.g., Monday) during the case month.

Secondary analyses using alternative heat measures showed that the association of high heat with higher rate of cardiovascular disease death in population analysis and higher odds of cardiovascular disease death in case-crossover analysis was observed using a 7-d heat index (the main exposure) and a 7-d mean of maximum daily temperatures (Figure 6). The corresponding effect estimates were 1.62 (95% CI: 1.25, 2.08) and 1.44 (95% CI: 1.12, 1.84) using data from the population model and 1.98 (95% CI: 1.41, 2.78) and 1.50 (95% CI: 1.10, 2.06) using the case-crossover designs. For both 2-d heat indices, this association was attenuated. Null or weak associations were observed between the alternative indicators of heat and noncardiovascular deaths.

Table 2. Characteristics of the participants (pooled data from two cohort studies in six Finnish cities, 2000–2018).

Study population characteristic	N (%)
All participants	363,754
Sex	
Men	103,846 (28.5)
Women	259,908 (71.5)
Age at baseline (y)	
Mean ± SD	35.3 ± 12.8
18–64 y	359,881 (98.9)
65–86 y	3,873 (1.1)
Age at the end of follow-up	
Mean ± SD	45.7 ± 15.4
18–64 y	311,251 (85.6)
65–86 y	52,503 (14.4)
Education at baseline	
Secondary or higher	326,650 (89.8)
Primary	37,083 (10.2)
Residential locations at baseline ^a	
Building: single-family home	
Yes	39,969 (11.3)
No	313,751 (88.7)
Missing	10,034
Neighborhood NDVI	
Mean ± SD	0.49 ± 0.14
High	248,188 (68.3)
Low	115,401 (31.7)
Missing	165
Neighborhood deprivation ^b	
Mean ± SD	-0.19 ± 0.68
Low	224,835 (62.2)
High	136,422 (37.8)
Missing	2,497
Heat island ^c	
No	237,704 (65.4)
Yes	126,050 (34.6)
Missing	0
Heat indices, 2000–2018 (mean ± SD)	
7-d heat index ^d	14.0 ± 4.1
7-d maximum temperature	19.0 ± 4.1
2-d heat index	13.8 ± 4.6
2-d maximum temperature	18.8 ± 4.6
Survey respondents (subsample)	
Obesity at baseline	
No	101,578 (80.6)
Yes	24,503 (19.4)
Missing	2,400
Ever-smoker at baseline	
No	73,243 (58.1)
Yes	52,915 (41.9)
Missing	2,323
High alcohol consumption at baseline	
No	96,118 (75.8)
Yes	30,596 (24.2)
Missing	1,767
Physical inactivity at baseline	
No	66,840 (19.4)
Yes	59,946 (52.7)
Missing	1,695
Risk behaviors	
0–1	76,899 (60.2)
2–4	50,913 (39.3)
Missing	669

Note: Figures are n (%) unless otherwise stated. NDVI, Normalized Difference Vegetation Index; SD, standard deviation.

^a750 m × 750 m resolution for greenness, and 250 m × 250 m resolution for other characteristics of residential location.

^bDeprivation in relation to grid-based national z-score.

^cPopulation density >500 per 250 m × 250 m grid area. During the follow-up, 205,116 participants lived in a heat island at some point.

^dAverage daily temperature level weighted by air humidity during a period of 7 d and nights.

Results from subgroup analyses were consistent across the population modeling and case-crossover study designs, although none of the differences in demographic, residential location, or

Table 3. Association of heat index with summertime all-cause and cause-specific mortality [pooled data from two cohort studies in six Finnish cities, 2000–2018, *N*(participants) = 363,754].

Cause of death	Heat index ^a	<i>N</i> (deaths)	<i>N</i> (person-summers) ^b	Rate (95% CI) ^c	RR (95% CI) ^d
All deaths	≤13	1,708	164,449	10.55 (10.01, 11.13)	1.01 (0.93, 1.09)
	14–15	836	78,801	10.49 (9.75, 11.28)	1.00 (Ref)
	16–17	731	72,620	10.26 (9.50, 11.07)	0.98 (0.89, 1.08)
	18–19	433	41,349	11.02 (9.99, 12.15)	1.05 (0.93, 1.18)
	20	109	10,449	10.90 (9.00, 13.19)	1.04 (0.85, 1.27)
	≥21	277	20,407	13.27 (11.69, 15.06)	1.27 (1.10, 1.46)
Cancer	≤13	646	164,449	3.15 (2.86, 3.46)	0.97 (0.85, 1.10)
	14–15	335	78,801	3.25 (2.88, 3.68)	1.00 (Ref)
	16–17	269	72,620	2.96 (2.60, 3.38)	0.91 (0.77, 1.07)
	18–19	178	41,349	3.57 (3.05, 4.18)	1.10 (0.91, 1.32)
	20	43	10,449	3.46 (2.55, 4.71)	1.06 (0.77, 1.47)
	≥21	103	20,407	4.04 (3.27, 4.99)	1.24 (0.98, 1.57)
Cardiovascular disease	≤13	410	164,449	1.84 (1.62, 2.08)	1.15 (0.97, 1.38)
	14–15	177	78,801	1.59 (1.34, 1.88)	1.00 (Ref)
	16–17	166	72,620	1.70 (1.43, 2.02)	1.07 (0.86, 1.32)
	18–19	93	41,349	1.73 (1.39, 2.16)	1.09 (0.84, 1.40)
	20	24	10,449	1.76 (1.17, 2.66)	1.11 (0.72, 1.71)
	≥21	79	20,407	2.72 (2.12, 3.48)	1.71 (1.29, 2.26)
External causes	≤13	281	164,449	2.13 (1.89, 2.41)	0.87 (0.71, 1.06)
	14–15	149	78,801	2.46 (2.09, 2.89)	1.00 (Ref)
	16–17	133	72,620	2.30 (1.93, 2.73)	0.94 (0.74, 1.18)
	18–19	74	41,349	2.28 (1.81, 2.87)	0.93 (0.70, 1.23)
	20	21	10,449	2.51 (1.63, 3.88)	1.02 (0.64, 1.63)
	≥21	36	20,407	2.28 (1.62, 3.21)	0.93 (0.64, 1.36)
Other causes	≤13	371	164,449	2.26 (2.01, 2.53)	1.05 (0.88, 1.26)
	14–15	175	78,801	2.14 (1.83, 2.52)	1.00 (Ref)
	16–17	163	72,620	2.24 (1.90, 2.64)	1.05 (0.84, 1.30)
	18–19	88	41,349	2.20 (1.77, 2.74)	1.03 (0.79, 1.33)
	20	21	10,449	2.01 (1.30, 3.10)	0.94 (0.59, 1.48)
	≥21	59	20,407	2.48 (1.89, 3.27)	1.16 (0.85, 1.58)

Note: CI, confidence interval; Ref, reference; RR, rate ratio.

^a7-d average.

^bFrom May to September.

^cRate per 10,000 person-summers adjusted for age, sex, and calendar year.

^dAge-, sex-, and calendar year-adjusted ratio of mortality and the 95% CIs by level of 7-d heat index.

lifestyle factors between subgroups achieved statistical significance (Figure 7). In analyses of data from both designs, there was a higher effect estimate for heat-related cardiovascular mortality in women, those ≥65 years of age, participants living in multiple-family homes, those who lived in regions of urban heat island effects, and individuals with high alcohol consumption or an unhealthy overall lifestyle. In case-crossover analyses only, a higher odds of heat-related cardiovascular mortality was also observed in individuals residing in deprived neighborhoods and those who were obese.

Future Summertime Heat-Related Cardiovascular Death Burden

In the whole of Finland, observed average increase in heat index between 1980–1999 and 2000–2019 is 0.56°C per decade. Projection for change in the heat index per decade until 2050 is 0.56°C if the current rate of climate change continues, 0.26°C per decade for the sustainable development scenario and 0.61°C per decade for the fossil-fueled development scenario (Figure 8A).

In our study population, the heat index was ≤14°C for 42.4% of summer days, within the 14–20°C range for 52.4% of summer days, and ≥21°C for 5.3% of summer days. If the current trend persists for the period 2030–2050, it is estimated that 30.5% of summer days will have a heat index of ≤14°C, 56.7% will fall in the 14–20°C range, and 12.8% will reach ≥21°C. The trends projected for our study population under a sustainable future scenario indicate a distribution of 36.4%, 55.7%, and 7.8% in the respective temperature categories. In contrast, in a

fossil-fueled future, the distribution shifts to 29.6%, 56.7%, and 13.8%.

These changes have an impact on the burden of summertime heat-related cardiovascular mortality, as indicated by the PAF (Figure 8B). In the period from 2000 to 2018, the PAF was 3.0% (95% CI: 1.2, 5.0) in our study population. Projections for 2030–2050 show PAF estimates of 7.1% (95% CI: 3.0, 11.5) under the current warming trend, 4.4% (95% CI: 1.8, 7.3) under the sustainable development scenario, and 7.6% (95% CI: 3.2, 12.3) under the fossil-fueled development scenario.

Table 5 shows the estimated summertime heat-related burden of cardiovascular deaths for the total 1.3 million population in the six cities in 2000–2019. This burden is only slightly higher, PAF = 3.2% (95% CI: 0.9, 6.1), than observed in the study participants (3.0%). A similar small difference is also evident in future projections for the years 2030–2050. According to the estimates from Statistics Finland, the population of the six cities is projected to reach 1.7 million, with a larger proportion of elderly individuals. Under the current warming trend, the PAF and the annual number of extra heat-related cardiovascular deaths are estimated to be PAF = 7.6% (95% CI: 2.8, 13.6) and *N*(deaths) = 278 (95% CI: 103, 497), respectively. In the sustainable development scenario, these figures are estimated to be PAF = 4.7% (95% CI: 1.7, 8.7) and *N*(deaths) = 174 (95% CI: 63, 318), whereas in the fossil-fueled development scenario, they are estimated to be PAF = 8.1% (95% CI: 3.0, 14.5) and *N*(deaths) = 298 (95% CI: 111, 530). For comparison, the PAF and the annual number of extra heat-related cardiovascular deaths for a more extreme future warming projection of 0°C and 1°C per decade are estimated to be PAF = 3.2% (95% CI: 1.2, 6.0) and *N*(deaths) = 118 (95% CI: 42, 218) and PAF = 16.2% (95% CI:

Table 4. Heat exposure and risk of association [RR (95% CI)] with summertime death from cardiovascular and noncardiovascular causes after serial adjustment [pooled data from two cohort studies in six Finnish cities, 2000–2018, *N*(participants) = 363,754].

Cause of death	Heat index (°C) ^a	<i>N</i> (deaths)	Model			
			1	2	3	4
All participants (<i>N</i> = 363,754)						
Cardiovascular disease	≤13	410	1.17 (0.98, 1.40)	1.15 (0.97, 1.38)	1.15 (0.97, 1.38)	1.14 (0.95, 1.36)
	14–15	177	1.00 (Ref)	1.00 (Ref)	1.00 (Ref)	1.00 (Ref)
	16–17	166	1.07 (0.86, 1.32)	1.07 (0.86, 1.32)	1.07 (0.86, 1.32)	1.06 (0.85, 1.32)
	18–19	93	1.07 (0.83, 1.39)	1.09 (0.84, 1.40)	1.09 (0.85, 1.41)	1.02 (0.78, 1.33)
	20	24	1.13 (0.73, 1.74)	1.11 (0.72, 1.71)	1.11 (0.72, 1.70)	1.09 (0.70, 1.70)
≥21	79	1.69 (1.28, 2.24)	1.71 (1.29, 2.26)	1.71 (1.29, 2.26)	1.70 (1.28, 2.27)	
Noncardiovascular	≤13	1,298	0.98 (0.89, 1.07)	0.97 (0.88, 1.06)	0.97 (0.88, 1.06)	0.97 (0.88, 1.06)
	14–15	659	1.00 (Ref)	1.00 (Ref)	1.00 (Ref)	1.00 (Ref)
	16–17	565	0.95 (0.85, 1.07)	0.95 (0.85, 1.07)	0.95 (0.85, 1.07)	0.96 (0.85, 1.07)
	18–19	340	1.03 (0.90, 1.18)	1.04 (0.91, 1.19)	1.04 (0.91, 1.19)	1.03 (0.89, 1.18)
	20	85	1.04 (0.82, 1.30)	1.02 (0.81, 1.28)	1.02 (0.81, 1.28)	1.05 (0.84, 1.33)
≥21	198	1.14 (0.96, 1.34)	1.15 (0.97, 1.35)	1.15 (0.97, 1.35)	1.14 (0.96, 1.36)	
Survey respondents (subsample, <i>N</i> = 128,481)						
Cardiovascular disease	≤13	95	1.51 (1.01, 2.26)	1.48 (0.99, 2.21)	1.50 (0.96, 2.32)	—
	14–15	32	1.00 (Ref)	1.00 (Ref)	1.00 (Ref)	—
	16–17	37	1.33 (0.83, 2.14)	1.34 (0.83, 2.16)	1.20 (0.71, 2.04)	—
	18–19	25	1.69 (0.99, 2.88)	1.71 (1.01, 2.92)	1.28 (0.67, 2.43)	—
	20	<10	1.04 (0.36, 2.97)	1.02 (0.36, 2.91)	0.95 (0.29, 3.19)	—
≥21	21	2.36 (1.32, 4.22)	2.39 (1.34, 4.28)	2.59 (1.38, 4.88)	—	
Noncardiovascular	≤13	323	1.04 (0.86, 1.26)	1.02 (0.84, 1.23)	1.07 (0.87, 1.32)	—
	14–15	163	1.00 (Ref)	1.00 (Ref)	1.00 (Ref)	—
	16–17	134	0.92 (0.73, 1.16)	0.93 (0.74, 1.16)	0.96 (0.74, 1.23)	—
	18–19	81	1.01 (0.77, 1.33)	1.02 (0.78, 1.34)	1.06 (0.78, 1.43)	—
	20	19	0.99 (0.61, 1.60)	0.98 (0.60, 1.58)	1.21 (0.74, 2.00)	—
≥21	57	1.37 (0.99, 1.89)	1.39 (1.01, 1.91)	1.39 (0.97, 1.99)	—	

Note: Adjustments to the model included the following: model 1: calendar year; model 2: calendar year, age, and sex; model 3: calendar year, age, sex, and education; model 4: calendar year, age, sex, education, type of building, greenness, neighborhood deprivation, and population density; model 5: calendar year, age, sex, education, type of building, greenness, neighborhood deprivation, population density, obesity, smoking, high alcohol intake, and physical inactivity. —, Not applicable; CI, confidence interval; Ref, reference; RR, rate ratio. ^a7-d average.

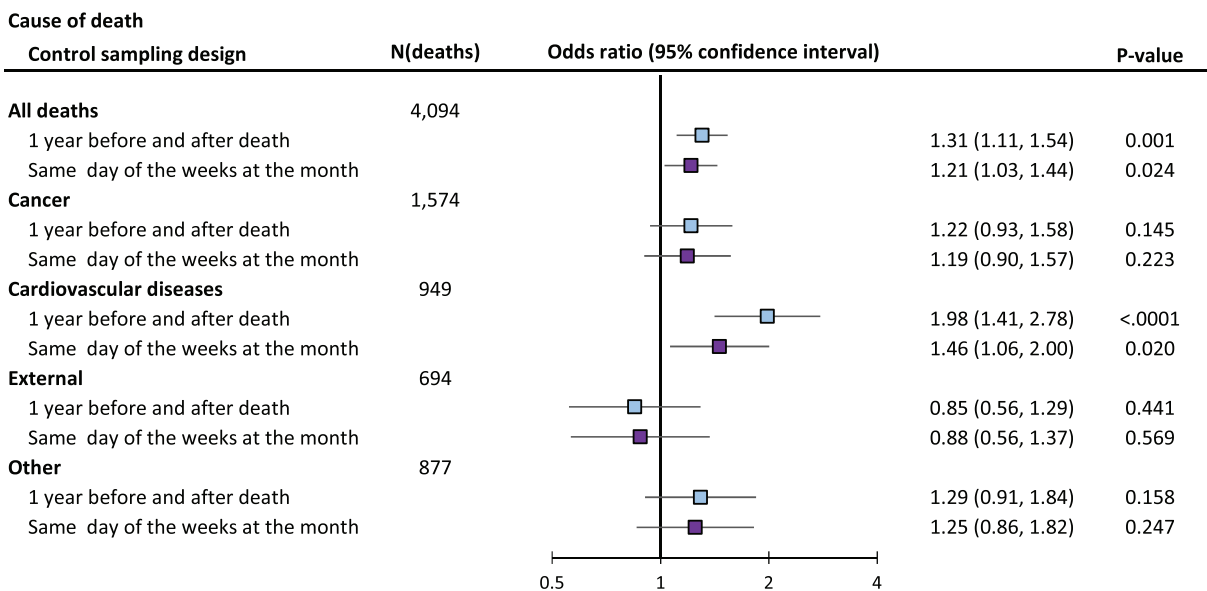


Figure 5. Case-crossover analysis of exposure to high heat index and risk of summertime all-cause and cause-specific mortality. Pooled individual-level data from two cohort studies in six Finnish cities, 2000–2018, were used. The number of participants in each analysis is the same as the number of deaths (range: 694–4,094). Conditional logistic regression with bidirectional control sampling was used for analysis. The analysis compares the odds of being exposed to high heat (≥21°C) in case time compared with control times. In the design “1 year before and after death,” control dates are 1 y before and after the date of death. In the design “Same day of the weeks at the month,” control dates are the same day of the week during the case month as the death day. All time-invariant covariates are controlled by the study design.

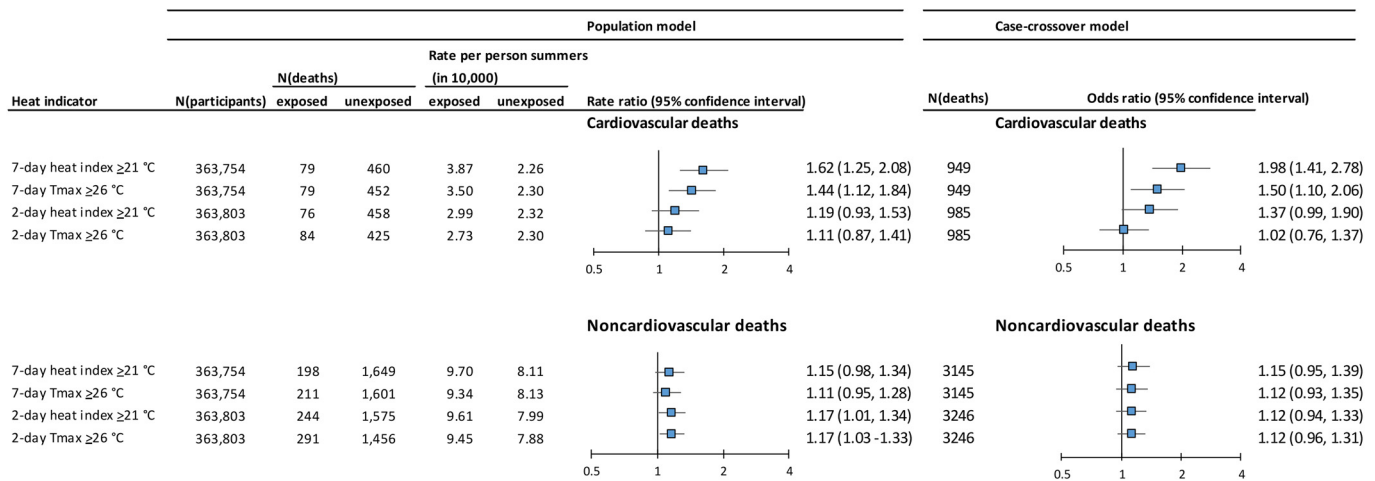


Figure 6. Heat exposure and risk of summertime cardiovascular and noncardiovascular death by heat indicator in population model and case-crossover analyses. Pooled individual-level data from two cohort studies in six Finnish cities, 2000–2018, were used. Population models are based on Poisson regression analysis. Mortality rate and age, sex, and calendar year-adjusted rate ratio for participants exposed to high heat index ($\geq 21^\circ\text{C}$) compared with those unexposed (heat index $14\text{--}20^\circ\text{C}$) are shown. Case-crossover models are based on conditional logistic regression with bidirectional control sampling. The analysis compares the odds of being exposed to high heat ($\geq 21^\circ\text{C}$) in case time (the date of death) compared with control times (1 y before and after the date of death). All time-invariant covariates are controlled by the study design. The number of participants in the case-crossover analysis is the same as the number of deaths. Note: Tmax, mean of daily maximum temperatures.

6.4, 27.1) and $N(\text{deaths}) = 594$ (95% CI: 235, 992), respectively. In all these comparisons, the relative and absolute difference in heat-related cardiovascular mortality burden between the most and least favorable warming trends is considerable.

Discussion

Findings for the six largest cities in Finland suggest that high ambient temperature is associated with moderately increased summertime cardiovascular disease mortality and slightly increased risk of total

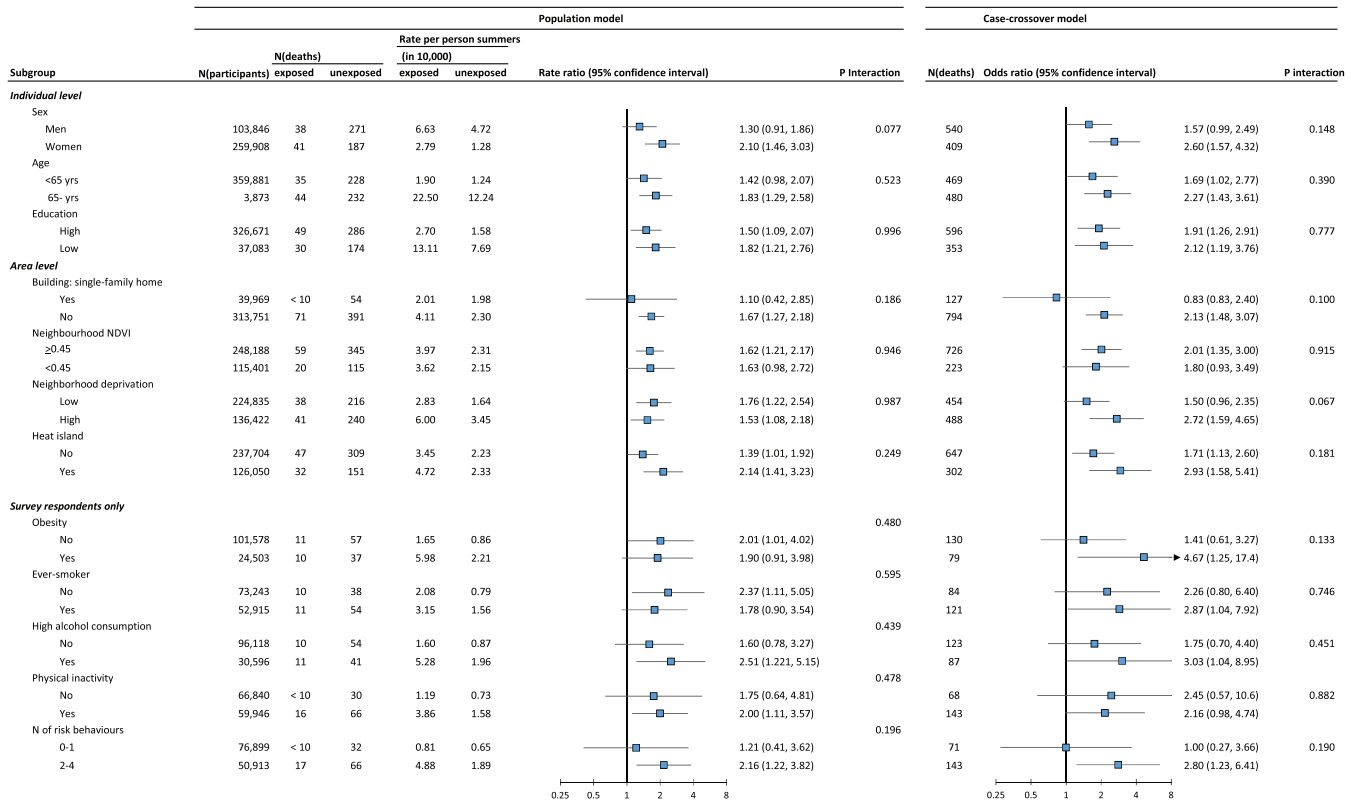


Figure 7. Heat exposure and risk of summertime cardiovascular death in population subgroups from a stratified population model and case-crossover analyses. Pooled individual-level data from two cohort studies in six Finnish cities, 2000–2018, were used. Population models and related tests for interaction are based on Poisson regression analysis. Mortality rate and age, sex, and calendar year-adjusted rate ratio for participants exposed to high heat index ($> 21^\circ\text{C}$) compared with those unexposed (heat index $14\text{--}20^\circ\text{C}$) are shown. Case-crossover models and related tests for interaction are based on conditional logistic regression with bidirectional control sampling. The analysis compares the odds of being exposed to high heat ($\geq 21^\circ\text{C}$) in case time (the date of death) compared with control times (1 y before and after the date of death). All time-invariant covariates are controlled by study design. The number of participants in case-crossover analysis is the same as the number of deaths. Note: NDVI, Normalized Difference Vegetation Index.

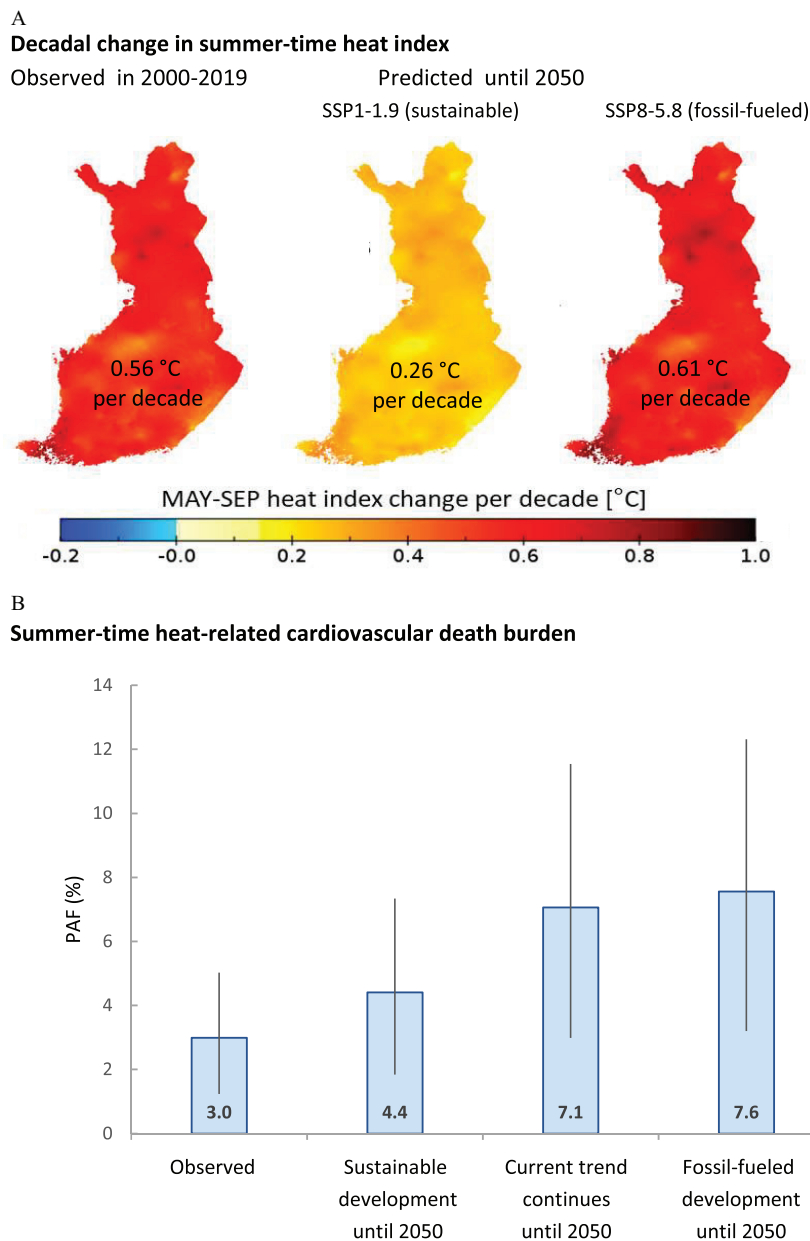


Figure 8. Observed and predicted burden of summertime heat-related cardiovascular death burden by climate change scenarios. (A) Observed decadal change in summertime heat index between 2000 and 2019 and projected decadal change in summertime heat index between 2030 and 2050 in Finland. (B) Summertime heat-related cardiovascular death burden as indicated by PAFs in participants living in six Finnish cities for 2000–2018 and 2030–2050 by climate change scenario. The whiskers in the bars represent 95% confidence intervals. Estimations in (B) are based on pooled individual-level data from two cohort studies in six Finnish cities, 2000–2018 ($N = 363,754$). Note: PAF, population attributable fraction; SEP, September; SSP, Shared Socioeconomic Pathway.

mortality. According to modeling of future heat-related mortality burden under two different climate change scenarios, the current summertime PAF of $\sim 3\%$ (95% CI: 1%, 6%) for fatal cardiovascular events will increase to 5% (95% CI: 2–9%) in the sustainable development scenario and to 8% (95% CI: 3–14%) in the fossil-fueled development scenario by 2030–2050. Thus, for cardiovascular mortality the estimated magnitude of increasing summertime mortality burden is almost two times greater if future climate change will be driven by fossil-fueled development compared with sustainable development.

To our knowledge, this study is one of few large-scale, high-resolution investigations using an individual-level daily based follow-up for location, temperature, humidity, and mortality. Thus, we were able to take into account participants' migrating to

new residential addresses during the 20-y exposure period and a large number of participant- and area-level covariates, including demographic characteristics, features of the residential building, neighborhood deprivation, heat islands, and health-related lifestyle factors. Our study also benefits from the national coverage of mortality registers.⁹⁵ The replication of epidemiological findings in multivariable-adjusted and case-crossover analyses strengthened the validity of our results that we used to draw projections from all summers between 1980 and 2019 to those between 2030 and 2050 under different global warming scenarios.

Our results on the association between heat and mortality are in accord with existing research, although the large variety of analytical designs, with alternative effect summaries, time periods, statistical modeling, and assumptions, makes direct comparisons difficult.

Table 5. Estimated burden of summer heat-related cardiovascular deaths in citizens of six Finnish cities by climate change scenario (pooled data from two cohort studies in six Finnish cities, 2000–2018).

	Year	Total adult population			Weighted	Weighted	Excess CVD (N)
		N	CVD deaths	Hot days (%) ^a	RR (95% CI) ^b	PAF (%) (95% CI) ^b	Deaths (95% CI)
Summers 2000–2018—observed	2010	1,306,928	2,040	5.3	1.668 (1.18, 2.34) ^c	3.19 (0.91, 6.14) ^c	65 (19, 125)
Summers 2030–2050—estimated	2040	1,759,468	3,665	—	—	—	—
Current warming trend	—	—	—	12.8	1.672 (1.24, 2.31) ^d	7.60 (2.81, 13.57) ^d	278 (103, 497)
SSP1-1.9 (sustainable scenario)	—	—	—	7.8	1.672 (1.24, 2.31) ^d	4.74 (1.72, 8.68) ^d	174 (63, 318)
SSP5-8.5 (fossil-fueled scenario)	—	—	—	13.8	1.672 (1.24, 2.31) ^d	8.13 (3.02, 14.46) ^d	298 (111, 530)
0°C change in temperature per decade	—	—	—	5.3	1.672 (1.24, 2.31) ^d	3.21 (1.15, 5.95) ^d	118 (42, 218)
1°C change in temperature per decade	—	—	—	29.7	1.672 (1.24, 2.31) ^d	16.20 (6.40, 27.07) ^d	594 (235, 992)

Note: —, Not applicable; CI, confidence interval; CVD, cardiovascular disease; PAF, population attributable fraction; Ref, reference; RR, rate ratio.

^aHeat index ≥ 21 during summer months.

^bRR and PAF for CVD deaths during summers estimated for heat index $\geq 21^\circ\text{C}$ vs. $14\text{--}20^\circ\text{C}$.

^cWeighted by age and sex distribution in the cities in 2010 (midpoint of 2000–2018).

^dWeighted by projected age and sex distribution in the cities in 2040 (midpoint of 2030–2050).

In accordance with reviews of the evidence, we found stronger association between heat index and cardiovascular mortality in women and people ≥ 65 years of age.^{11,96–99} The observed associations with cardiovascular mortality in subgroup analyses also highlighted higher risk in study participants living in regions with potential urban heat island effects—a finding that is consistent with previous studies, suggesting that factors characterizing heat islands, such as high population density and reduced urban vegetation, increase vulnerability to heat.^{100,101} The finding that the link between heat index and cardiovascular mortality was highest among those individuals with the least healthy lifestyles is novel yet biologically plausible.¹⁰²

The mechanisms underlying the observed associations remain unclear. Heat exhaustion or heat strokes (defined as a core temperature of $>40.6^\circ\text{C}$) can cause heart failure, but studies suggest that most heat-related deaths are not attributable to heat stroke, and this is particularly true in Finland where extreme ambient temperatures are extremely rare.^{103,104} Heat represents an acute stressor that may act on preexisting or subclinical vascular disease and, consistently with this, increased risk of heat-related mortality has often been observed among people with diabetes, hyperlipidemia, or cardiovascular disease.^{104–106} Heat-induced increases in body temperature activate the heat loss responses of cutaneous vasodilation and sweating, which reduce peripheral vascular resistance and central blood volume, require greater cardiac contractility and cardiac output, and increase heart rate. In vulnerable people, the resulting greater cardiovascular strain lowers the arrhythmic threshold and may predispose to ischemia and major adverse cardiac events.⁹ In addition, heat-induced inflammatory response can increase risk of thrombosis.⁹ In terminally ill individuals, high temperature, as a stressor, predisposes to organ failure.

Prior predictions of future heat-related mortality have been inconsistent and usually based on aggregate data. An analysis of 44 large U.S. cities with metropolitan areas exceeding 1 million residents predicted that climate change for the years 2020–2050 will dramatically increase summer mortality and slightly decrease winter mortality, even if people acclimatize to the increased warmth.¹⁰⁷ Another study, using aggregate data from daily deaths of older people living in North and South Finland, German (Baden Württemberg), Netherlands, the UK (London), North Italy, and Greece (Athens), came to an opposite conclusion.¹⁰⁸ The investigators found little differences in annual heat-related mortality between regions with hot summers compared with cold regions. Assuming this cross-sectional finding applies to longitudinal predictions, they suggested people can be expected to adjust to the global warming predicted for the next decades with little sustained increase in annual heat-related mortality. In accordance with our findings, other reports have favored views emphasizing future increases in heat-related mortality. These studies have used various sources of data for projections, including those collected from

Europe,^{19,20} 15 European cities,¹⁰⁹ a large city in the Netherlands,²¹ New York City,²² 10 large metropolitan areas in the United States,²³ Central and Southern America,¹⁹ Southeast Asia,¹⁹ 7 large cities of South Korea,²⁴ Beijing,²⁵ a Chinese coastal city,²⁶ and urban and rural counties in China.²⁷

We estimated the future mortality burden under two climate change scenarios using adapted projections of preceding temperature shift from 1980–1999 to 2000–2018 and including Statistical Finland projections for demographic changes in the studied six cities.^{91–94} In predicting the number of heat-related cardiovascular deaths in 2030–2050, we controlled for the hot model bias^{89,90} and took into account both population growth and population aging because adverse heat-related effects are more pronounced in older people—the age group in Finland, and many other countries, that will increase most in absolute numbers in future.^{92–94} If the current warming trend continues, the estimated increase in the number of future summertime heat-related cardiovascular deaths is 4-fold. This increase would be smaller, <3 -fold under the sustainable climate change scenario, but more than 4.5-fold assuming a fossil-fueled future. Modeling of more extreme changes to the current warming trend, such as temperature increases of 0°C and 1°C per decade, led to greater differences in the burden of heat-related cardiovascular mortality between the most and least favorable climate scenarios.

Although the present findings on a greater burden of summertime cardiovascular disease mortality in urban heat islands is intuitive and in accord with other results,^{110,111} they should be interpreted cautiously. First, the measurement of urban heat islands was based on population density. It therefore missed important factors that cause the urban heat island effect, such as impervious surfaces or anthropogenic heat emission,¹¹² although associations of our urban heat island measurement with higher temperatures and lower NDVI were seen in the validation substudy. Second, our estimates of mortality risk accounted for uncertainty in the heat-mortality associations, but not the uncertainty in future climate scenarios, which has been taken into account in some previous studies not based on individual-level cohort data.^{18,19} To evaluate the uncertainty in warming trends of the sustainable development and fossil-fueled scenarios, we predicted mortality burden separately for 0°C and 1°C increases in temperature per decade. These approximately represent the lower and upper ends of the 95% CrIs for the two global warming scenarios. Third, in the modeling of the future burden of heat-related cardiovascular deaths, it was not possible to consider the influence of increases in heat islands within urban areas owing to the lack of relevant data, a limitation shared by several other studies in the field.^{17,112–114} This could have contributed to an underestimation of true effects because the impact of warming induced by urbanization can be even greater than the impact of climate change.^{115,116} Other potentially health-related climate data not available for this study include air pollution,

average wind speed, and wind direction,^{12,117,118} although recent multi-model mean results suggest close to zero changes in wind speed in Finland over time.¹¹⁹ It also remains unknown how future improvements in health care, air conditioning of homes and vehicles, and physiological acclimatization will affect the ability of humans to adapt to higher temperatures.

Although heat-related death burden varies geographically, increased heat-related mortality is evident on every inhabited continent with different weather and geographic conditions.¹⁸ Our study was based on data from six large cities in Finland, a cold-climate Northern-latitude country. The findings may not be generalizable to rural areas in Finland or other countries with different weather and geographic conditions. The vast majority of the participants were employed and relatively young, with the mean age at death being 60 y. This implies that the population segments most vulnerable to heat stress, such as people with low incomes, members of minority groups, older adults, and people with chronic diseases and disabilities,^{102,120} were underrepresented in these data. Thus, we may have underestimated the heat-associated death burden. Furthermore, the climate in Finland varies between subarctic or humid continental, and summers are typically mild.²⁹ Because of this relatively low countrywide heat exposure, one would expect the burden of heat-related deaths to be lower in Finland than in those regions with hotter summers. This may, however, be only partially true. Populations tend to adjust to local temperatures over centuries and millennia and, thus, mortality risk is not a simple function of the heat index, which applies universally.^{118,121}

This study focused on heat-related mortality during summers, and further research covering cold-related deaths during winters is needed for an overall evaluation of global warming. This would require control for time-varying individual-level covariates relevant for cold-related health effects (e.g., variation in snow cover, ice, and light), which, of course, differ from those for heat-related impacts. The potential interactions between heat- and cold-related biological mechanisms add a further layer of complexity to such analysis.

In conclusion, individual-level daily based spatiotemporal data in citizens from Finland suggest that climate change will increase heat-related cardiovascular mortality in urban-dwelling populations. The increase in summertime death burden from cardiovascular diseases will be >1.5 times greater if future human-induced global warming follows the fossil-fueled development rather than sustainable development scenario. These findings support the need for more ambitious mitigation and adaptation strategies to minimize the public health impacts of climate change.

Acknowledgments

Authors' contributions are as follows: formulating research questions—M.K., J.P., and J.V.; designing the study—M.K., J.P., and J.V.; data preparation—J.P., J.S., J.K., J.M., A.-I.P., and K.N.; statistical analysis—J.P., J.S., J.K., J.M., A.-I.P., and K.N.; manuscript writing and revising—M.K., G.D.B., J.P., J.S., S.T.N., J.M., K.N., J.E., S.B.S., A.-I.P., S.S., J.K., and J.V.; and verifying the underlying data—J.P. and J.V.

This study was supported by the Academy of Finland (329240; 329241; 329235). M.K. was supported by the Wellcome Trust (221854/Z/20/Z), the UK Medical Research Council (MR/S011676/1), the U.S. National Institute on Aging (NIH; R01AG056477), and the Academy of Finland (329202, 350426). G.D.B. was supported by the UK Medical Research Council (MR/P023444/1) and the U.S. National Institute on Aging (1R56AG052519-01; 1R01AG052519-01A1). J.P. and S.T.N. were supported by the Finnish Work Environment Fund (190424) and the Academy of Finland (329202). J.K. and J.S. are grateful for the support by the University of Turku Geography Division and the City of Turku for maintaining the TURCLIM network. S.S. was supported by the Academy of Finland

(332030). J.V. was supported by the Academy of Finland (321409). The funders of the study had no role in study design, data collection, data analysis, data interpretation, or writing of the report.

Data sharing statement: the statistical code is provided in the Supplemental Material. Climate data sets are publicly available and are specified in the statistical code (https://colab.research.google.com/drive/1ZF-2d9Fbs0Uzh5_jNtiwRH6tOfzNDxMN, <https://colab.research.google.com>). The pseudonymized questionnaire data used in the Finnish Public Sector study are available for bona fide researchers by request to the investigators (jenni.ervasti@ttl.fi) and after approval of the Finnish Institute of Occupational Health scientific committees. Linked electronic health records additionally require separate permission from the National Institute of Health and Welfare and Statistics Finland.

References

1. Costello A, Abbas M, Allen A, Ball S, Bell S, Bellamy R, et al. 2009. Managing the health effects of climate change: *Lancet* and University College London Institute for Global Health Commission. *Lancet* 373(9676):1693–1733, PMID: 19447250, [https://doi.org/10.1016/S0140-6736\(09\)60935-1](https://doi.org/10.1016/S0140-6736(09)60935-1).
2. Atwoli L, Baqui AH, Benfield T, Bosurgi R, Godlee F, Hancocks S, et al. 2021. Call for emergency action to limit global temperature increases, restore biodiversity, and protect health. *PLoS Med* 18(9):e1003755, PMID: 34492002, <https://doi.org/10.1371/journal.pmed.1003755>.
3. Rocque RJ, Beaudoin C, Ndjaboue R, Cameron L, Poirier-Bergeron L, Poulin-Rheault RA, et al. 2021. Health effects of climate change: an overview of systematic reviews. *BMJ Open* 11(6):e046333, PMID: 34108165, <https://doi.org/10.1136/bmjopen-2020-046333>.
4. Bunker A, Wildenhain J, Vandenbergh A, Henschke N, Rocklöv J, Hajat S, et al. 2016. Effects of air temperature on climate-sensitive mortality and morbidity outcomes in the elderly: a systematic review and meta-analysis of epidemiological evidence. *EBioMedicine* 6:258–268, PMID: 27211569, <https://doi.org/10.1016/j.ebiom.2016.02.034>.
5. Cheng J, Xu Z, Bambrick H, Prescott V, Wang N, Zhang Y, et al. 2019. Cardiorespiratory effects of heatwaves: a systematic review and meta-analysis of global epidemiological evidence. *Environ Res* 177:108610, PMID: 31376629, <https://doi.org/10.1016/j.envres.2019.108610>.
6. Chen K, Breitner S, Wolf K, Hampel R, Meisinger C, Heier M, et al. 2019. Temporal variations in the triggering of myocardial infarction by air temperature in Augsburg, Germany, 1987–2014. *Eur Heart J* 40(20):1600–1608, PMID: 30859207, <https://doi.org/10.1093/eurheartj/ehz116>.
7. Gostimirovic M, Novakovic R, Rajkovic J, Djokic V, Terzic D, Putnik S, et al. 2020. The influence of climate change on human cardiovascular function. *Arch Environ Occup Health* 75(7):406–414, PMID: 32200732, <https://doi.org/10.1080/19338244.2020.1742079>.
8. Bai L, Li Q, Wang J, Lavigne E, Gasparrini A, Copes R, et al. 2018. Increased coronary heart disease and stroke hospitalisations from ambient temperatures in Ontario. *Heart* 104(8):673–679, PMID: 29101264, <https://doi.org/10.1136/heartjnl-2017-311821>.
9. Chaselings GK, Iglesias-Grau J, Juneau M, Nigam A, Kaiser D, Gagnon D. 2021. Extreme heat and cardiovascular health: what a cardiovascular health professional should know. *Can J Cardiol* 37(11):1828–1836, PMID: 34802857, <https://doi.org/10.1016/j.cjca.2021.08.008>.
10. Sun Z, Chen C, Xu D, Li T. 2018. Effects of ambient temperature on myocardial infarction: a systematic review and meta-analysis. *Environ Pollut* 241:1106–1114, PMID: 30029319, <https://doi.org/10.1016/j.envpol.2018.06.045>.
11. Liu J, Varghese BM, Hansen A, Zhang Y, Driscoll T, Morgan G, et al. 2022. Heat exposure and cardiovascular health outcomes: a systematic review and meta-analysis. *Lancet Planet Health* 6(6):e484–e495, PMID: 35709806, [https://doi.org/10.1016/S2542-5196\(22\)00117-6](https://doi.org/10.1016/S2542-5196(22)00117-6).
12. Khraishah H, Alahmad B, Ostergard RL Jr, AlAshqar A, Albaghdadi M, Vellanki N, et al. 2011. Climate change and cardiovascular disease: implications for global health. *Nat Rev Cardiol* 19(12):798–812, PMID: 35672485, <https://doi.org/10.1038/s41569-022-00720-x>.
13. Basagaña X, Sartini C, Barrera-Gómez J, Davdand P, Cunillera J, Ostro B, et al. 2011. Heat waves and cause-specific mortality at all ages. *Epidemiology* 22(6):765–772, PMID: 21968768, <https://doi.org/10.1097/EDE.0b013e31823031c5>.
14. Burkart KG, Brauer M, Aravkin AY, Godwin WW, Hay SI, He J, et al. 2021. Estimating the cause-specific relative risks of non-optimal temperature on daily mortality: a two-part modelling approach applied to the Global Burden of Disease Study. *Lancet* 398(10301):685–697, PMID: 34419204, [https://doi.org/10.1016/S0140-6736\(21\)01700-1](https://doi.org/10.1016/S0140-6736(21)01700-1).

15. Eyring V, Bony S, Meehl GA, Senior CA, Stevens B, Stouffer RJ, et al. 2016. Overview of the Coupled Model Intercomparison Project Phase 6 (CMIP6) experimental design and organization. *Geosci Model Dev* 9(5):1937–1958, <https://doi.org/10.5194/gmd-9-1937-2016>.
16. Riahi K, van Vuuren DP, Kriegler E, Edmonds J, O'Neill BC, Fujimori S, et al. 2017. The Shared Socioeconomic Pathways and their energy, land use, and greenhouse gas emissions implications: an overview. *Glob Environ Change* 42:153–168, <https://doi.org/10.1016/j.gloenvcha.2016.05.009>.
17. Sanderson M, Arbutnott K, Kovats S, Hajat S, Falloon P. 2017. The use of climate information to estimate future mortality from high ambient temperature: a systematic literature review. *PLoS One* 12(7):e0180369, PMID: 28686743, <https://doi.org/10.1371/journal.pone.0180369>.
18. Vicedo-Cabrera AM, Scovronick N, Sera F, Royé D, Schneider R, Tobias A, et al. 2021. The burden of heat-related mortality attributable to recent human-induced climate change. *Nat Clim Chang* 11(6):492–500, PMID: 34221128, <https://doi.org/10.1038/s41558-021-01058-x>.
19. Gasparini A, Guo Y, Sera F, Vicedo-Cabrera AM, Huber V, Tong S, et al. 2017. Projections of temperature-related excess mortality under climate change scenarios. *Lancet Planet Health* 1(9):e360–e367, PMID: 29276803, [https://doi.org/10.1016/S2542-5196\(17\)30156-0](https://doi.org/10.1016/S2542-5196(17)30156-0).
20. Ballester J, Robine JM, Herrmann FR, Rodó X. 2011. Long-term projections and acclimatization scenarios of temperature-related mortality in Europe. *Nat Commun* 2:358, PMID: 21694706, <https://doi.org/10.1038/ncomms1360>.
21. Martinez GS, Diaz J, Hooyberghs H, Lauwaet D, De Ridder K, Linares C, et al. 2018. Heat and health in Antwerp under climate change: projected impacts and implications for prevention. *Environ Int* 111:135–143, PMID: 29207285, <https://doi.org/10.1016/j.envint.2017.11.012>.
22. Petkova EP, Vink JK, Horton RM, Gasparini A, Bader DA, Francis JD, et al. 2017. Towards more comprehensive projections of urban heat-related mortality: estimates for New York City under multiple population, adaptation, and climate scenarios. *Environ Health Perspect* 125(1):47–55, PMID: 27337737, <https://doi.org/10.1289/EHP166>.
23. Weinberger KR, Haykin L, Eliot MN, Schwartz JD, Gasparini A, Wellenius GA. 2017. Projected temperature-related deaths in ten large U.S. metropolitan areas under different climate change scenarios. *Environ Int* 107:196–204, PMID: 28750225, <https://doi.org/10.1016/j.envint.2017.07.006>.
24. Lee JY, Kim H. 2016. Projection of future temperature-related mortality due to climate and demographic changes. *Environ Int* 94:489–494, PMID: 27316627, <https://doi.org/10.1016/j.envint.2016.06.007>.
25. Li T, Horton RM, Bader DA, Liu F, Sun Q, Kinney PL. 2018. Long-term projections of temperature-related mortality risks for ischemic stroke, hemorrhagic stroke, and acute ischemic heart disease under changing climate in Beijing, China. *Environ Int* 112:1–9, PMID: 29241068, <https://doi.org/10.1016/j.envint.2017.12.006>.
26. Gu S, Zhang L, Sun S, Wang X, Lu B, Han H, et al. 2020. Projections of temperature-related cause-specific mortality under climate change scenarios in a coastal city of China. *Environ Int* 143:105889, PMID: 32619913, <https://doi.org/10.1016/j.envint.2020.105889>.
27. Chen K, Horton RM, Bader DA, Lesk C, Jiang L, Jones B, et al. 2017. Impact of climate change on heat-related mortality in Jiangsu Province, China. *Environ Pollut* 224:317–325, PMID: 28237309, <https://doi.org/10.1016/j.envpol.2017.02.011>.
28. Maclure M, Mittleman MA. 2000. Should we use a case-crossover design? *Annu Rev Public Health* 21:193–221, PMID: 10884952, <https://doi.org/10.1146/annurev.publhealth.21.1.193>.
29. Ruosteenoja K, Jylhä K, Kämäräinen M. 2016. Climate projections for Finland under the RCP forcing scenarios. *Geophysica* 51(1):17–50.
30. Ruosteenoja K, Räisänen J. 2021. Evolution of observed and modelled temperatures in Finland in 1901–2018 and potential dynamical reasons for the differences. *Int J Climatol* 41(5):3374–3390, <https://doi.org/10.1002/joc.7024>.
31. IPCC (Intergovernmental Panel on Climate Change). 2022. *Climate Change 2021: The Physical Science Basis. Contribution of Working Group I to the Sixth Assessment Report of the Intergovernmental Panel on Climate Change*. Masson-Delmotte V, Zhai P, Pirani A, et al., eds. Cambridge, UK: Cambridge University Press.
32. Räisänen J. 2019. Effect of atmospheric circulation on recent temperature changes in Finland. *Clim Dyn* 53(9–10):5675–5687, <https://doi.org/10.1007/s00382-019-04890-2>.
33. Korkeila K, Suominen S, Ahvenainen J, Ojanlatva A, Rautava P, Helenius H, et al. 2011. Non-response and related factors in a nation-wide health survey. *Eur J Epidemiol* 17(11):991–999, PMID: 12380710, <https://doi.org/10.1023/a:1020016922473>.
34. Kivimäki M, Lawlor DA, Davey Smith G, Kouvonen A, Virtanen M, Elovainio M, et al. 2007. Socioeconomic position, co-occurrence of behavior-related risk factors, and coronary heart disease: the Finnish Public Sector Study. *Am J Public Health* 97(5):874–879, PMID: 17395837, <https://doi.org/10.2105/AJPH.2005.078691>.
35. Aalto J, Pirinen P, Jylhä K. 2016. New gridded daily climatology of Finland: permutation-based uncertainty estimates and temporal trends in climate. *J Geophys Res* 121(8):3807–3823, <https://doi.org/10.1002/2015JD024651>.
36. Barnett AG, Tong S, Clements ACA. 2010. What measure of temperature is the best predictor of mortality? *Environ Res* 110(6):604–611, PMID: 20519131, <https://doi.org/10.1016/j.envres.2010.05.006>.
37. Anderson GB, Bell ML, Peng RD. 2013. Methods to calculate the heat index as an exposure metric in environmental health research. *Environ Health Perspect* 121(10):1111–1119, PMID: 23934704, <https://doi.org/10.1289/ehp.1206273>.
38. Armstrong B, Sera F, Vicedo-Cabrera AM, Abrutzky R, Åström DO, Bell ML, et al. 2019. The role of humidity in associations of high temperature with mortality: a multicountry, multicity study. *Environ Health Perspect* 127(9):097007, PMID: 31553655, <https://doi.org/10.1289/EHP5430>.
39. Khatana SAM, Werner RM, Groeneveld PW. 2022. Association of extreme heat and cardiovascular mortality in the United States: a county-level longitudinal analysis from 2008 to 2017. *Circulation* 146(3):249–261, PMID: 35726635, <https://doi.org/10.1161/CIRCULATIONAHA.122.060746>.
40. Kim H, Ha JS, Park J. 2006. High temperature, heat index, and mortality in 6 major cities in South Korea. *Arch Environ Occup Health* 61(6):265–270, PMID: 17967749, <https://doi.org/10.3200/AEOH.61.6.265-270>.
41. Sung TI, Wu PC, Lung SC, Lin CY, Chen MJ, Su HJ. 2013. Relationship between heat index and mortality of 6 major cities in Taiwan. *Sci Total Environ* 442:275–281, PMID: 23178831, <https://doi.org/10.1016/j.scitotenv.2012.09.068>.
42. National Weather Service. 2022. The Heat Index Equation. https://www.wpc.ncep.noaa.gov/html/heatindex_equation.shtml [accessed 23 January 2022].
43. Chen R, Yin P, Wang L, Liu C, Niu Y, Wang W, et al. 2018. Association between ambient temperature and mortality risk and burden: time series study in 272 main Chinese cities. *BMJ* 363:k4306, PMID: 30381293, <https://doi.org/10.1136/bmj.k4306>.
44. Ishigami A, Hajat S, Kovats RS, Bisanti L, Rognoni M, Russo A, et al. 2008. An ecological time-series study of heat-related mortality in three European cities. *Environ Health* 7:5, PMID: 18226218, <https://doi.org/10.1186/1476-069X-7-5>.
45. Ruuhela R, Votsis A, Kukkonen J, Jylhä K, Kankaanpää S, Perrels A. 2021. Temperature-related mortality in Helsinki compared to its surrounding region over two decades, with special emphasis on intensive heat waves. *Atmosphere* (Basel) 12(1):46, <https://doi.org/10.3390/atmos12010046>.
46. Kivimäki M, Batty GD, Pentti J, Nyberg ST, Lindbohm JV, Ervasti J, et al. 2021. Modifications to residential neighbourhood characteristics and risk of 79 common health conditions: a prospective cohort study. *Lancet Public Health* 6(6):e396–e407, PMID: 34051163, [https://doi.org/10.1016/S2468-2667\(21\)00066-9](https://doi.org/10.1016/S2468-2667(21)00066-9).
47. Lahdenperä M, Galante L, Gonzales-Inca C, Vahtera J, Pentti J, Rautava S, et al. 2023. Residential green environments are associated with human milk oligosaccharide diversity and composition. *Sci Rep* 13(1):216, PMID: 36604578, <https://doi.org/10.1038/s41598-022-27317-1>.
48. Nyberg ST, Singh-Manoux A, Pentti J, Madsen IEH, Sabia S, Alfredsson L, et al. 2020. Association of healthy lifestyle with years lived without major chronic diseases. *JAMA Intern Med* 180(5):760–768, PMID: 32250383, <https://doi.org/10.1001/jamainternmed.2020.0618>.
49. World Health Organization. 2019. ICD-10 Version:2019. <https://icd.who.int/browse10/2019/en#!> [accessed 23 January 2022].
50. van Vuuren DP, Stehfest E, Gernaat DEHJ, Doelman JC, van den Berg M, Harmsen M, et al. 2017. Energy, land-use and greenhouse gas emissions trajectories under a green growth paradigm. *Glob Environ Change* 42:237–250, <https://doi.org/10.1016/j.gloenvcha.2016.05.008>.
51. Kriegler E, Bauer N, Popp A, Humpenöder F, Leimbach M, Strefler J, et al. 2017. Fossil-fueled development (SSP5): an energy and resource intensive scenario for the 21st century. *Glob Environ Change* 42:297–315, <https://doi.org/10.1016/j.gloenvcha.2016.05.015>.
52. Dunne JP, Horowitz LW, Adcroft AJ, Ginoux P, Held IM, John JG, et al. 2020. The GFDL Earth System Model Version 4.1 (GFDL-ESM 4.1): overall coupled model description and simulation characteristics. *J Adv Model Earth Syst* 12(11):e2019MS002015, <https://doi.org/10.1029/2019MS002015>.
53. Krasting JP, John JG, Blanton C, McHugh C, Nikonov S, Radhakrishnan A, et al. 2018. NOAA-GFDL GFDL-ESM4 model output prepared for CMIP6 CMIP historical. Earth System Grid Federation. <https://doi.org/10.22033/ESGF/CMIP6.8597>.
54. John JG, Blanton C, McHugh C, Radhakrishnan A, Rand K, Vahlenkamp H, et al. 2018. NOAA-GFDL GFDL-ESM4 model output prepared for CMIP6 ScenarioMIP ssp119. Earth System Grid Federation. <https://doi.org/10.22033/ESGF/CMIP6.8683>.
55. John JG, Blanton C, McHugh C, Radhakrishnan A, Rand K, Vahlenkamp H, et al. 2018. NOAA-GFDL GFDL-ESM4 model output prepared for CMIP6 ScenarioMIP ssp585. Earth System Grid Federation. <https://doi.org/10.22033/ESGF/CMIP6.8706>.
56. Boucher O, Servonnat J, Albright AL, Aumont O, Balkanski Y, Bastrikov V, et al. 2020. Presentation and evaluation of the IPSL-CM6A-LR climate model. *J Adv Model Earth Syst* 12(7):e2019MS002010, <https://doi.org/10.1029/2019MS002010>.
57. Boucher O, Denvil S, Levassieur G, Cozic A, Caubel A, Foujols MA, et al. 2018. IPSL-CM6A-LR model output prepared for CMIP6 CMIP historical. Earth System Grid Federation. <https://doi.org/10.22033/ESGF/CMIP6.5195>.

58. Boucher O, Denvil S, Levavasseur G, Cozic A, Caubel A, Foujols MA, et al. 2019. IPSL IPSL-CM6A-LR model output prepared for CMIP6 ScenarioMIP ssp585. Earth System Grid Federation. <https://doi.org/10.22033/ESGF/CMIP6.5271>.
59. Boucher O, Denvil S, Levavasseur G, Cozic A, Caubel A, Foujols MA, et al. 2019. IPSL IPSL-CM6A-LR model output prepared for CMIP6 ScenarioMIP ssp119. Earth System Grid Federation. <https://doi.org/10.22033/ESGF/CMIP6.5261>.
60. Tatebe H, Ogura T, Nitta T, Komuro Y, Ogochi K, Takemura T, et al. 2019. Description and basic evaluation of simulated mean state, internal variability, and climate sensitivity in MIROC6. *Geosci Model Dev* 12(7):2727–2765, <https://doi.org/10.5194/gmd-12-2727-2019>.
61. Tatebe H, Watanabe M. 2018. MIROC MIROC6 model output prepared for CMIP6 CMIP historical. Earth System Grid Federation. <https://doi.org/10.22033/ESGF/CMIP6.5603>.
62. Shiogama H, Abe M, Tatebe H. 2019. MIROC MIROC6 model output prepared for CMIP6 ScenarioMIP ssp119. Earth System Grid Federation. <https://doi.org/10.22033/ESGF/CMIP6.5741>.
63. Shiogama H, Abe M, Tatebe H. 2019. MIROC MIROC6 model output prepared for CMIP6 ScenarioMIP ssp585. Earth System Grid Federation. <https://doi.org/10.22033/ESGF/CMIP6.5771>.
64. Yukimoto S, Kawai H, Koshiro T, Oshima N, Yoshida K, Urakawa S, et al. 2019. The Meteorological Research Institute Earth System Model version 2.0, MRI-ESM2.0: description and basic evaluation of the physical component. *J Meteorol Soc Japan* 97:931–965, <https://doi.org/10.2151/jmsj.2019-051>.
65. Yukimoto S, Koshiro T, Kawai H, Oshima N, Yoshida K, Urakawa S, et al. 2019. MRI MRI-ESM2.0 model output prepared for CMIP6 CMIP historical. Earth System Grid Federation. <https://doi.org/10.22033/ESGF/CMIP6.6842>.
66. Yukimoto S, Koshiro T, Kawai H, Oshima N, Yoshida K, Urakawa S, et al. 2019. MRI MRI-ESM2.0 model output prepared for CMIP6 ScenarioMIP ssp119. Earth System Grid Federation. <https://doi.org/10.22033/ESGF/CMIP6.6908>.
67. Yukimoto S, Koshiro T, Kawai H, Oshima N, Yoshida K, Urakawa S, et al. 2019. MRI MRI-ESM2.0 model output prepared for CMIP6 ScenarioMIP ssp585. Earth System Grid Federation. <https://doi.org/10.22033/ESGF/CMIP6.6929>.
68. Swart NC, Cole JNS, Kharin VV, Lazare M, Scinocca JF, Gillett NP, et al. 2019. The Canadian Earth System Model version 5 (CanESM5.0.3). *Geosci Model Dev* 12(11):4823–4873, <https://doi.org/10.5194/gmd-12-4823-2019>.
69. Swart NC, Cole JNS, Kharin VV, Lazare M, Scinocca JF, Gillett NP, et al. 2019. CCCma CanESM5 model output prepared for CMIP6 CMIP historical. Earth System Grid Federation. <https://doi.org/10.22033/ESGF/CMIP6.3610>.
70. Swart NC, Cole JNS, Kharin VV, Lazare M, Scinocca JF, Gillett NP, et al. 2019. CCCma CanESM5 model output prepared for CMIP6 ScenarioMIP ssp119. Earth System Grid Federation. <https://doi.org/10.22033/ESGF/CMIP6.3682>.
71. Swart NC, Cole JNS, Kharin VV, Lazare M, Scinocca JF, Gillett NP, et al. 2019. CCCma CanESM5 model output prepared for CMIP6 ScenarioMIP ssp585. Earth System Grid Federation. <https://doi.org/10.22033/ESGF/CMIP6.3696>.
72. Rong XY, Li J, Chen HM, Xin YF, Su JZ, Hua JL, et al. 2019. Introduction of CAMS-CSM model and its participation in CMIP6[J]. *Clim Change Res* 15:540–544, <https://doi.org/10.12006/j.issn.1673-1719.2019.186>.
73. Rong X. 2019. CAMS CAMS-CSM1.0 model output prepared for CMIP6 CMIP historical. Earth System Grid Federation. <https://doi.org/10.22033/ESGF/CMIP6.9754>.
74. Rong X. 2019. CAMS CAMS-CSM1.0 model output prepared for CMIP6 ScenarioMIP ssp585. Earth System Grid Federation. <https://doi.org/10.22033/ESGF/CMIP6.11052>.
75. Rong X. 2019. CAMS CAMS-CSM1.0 model output prepared for CMIP6 ScenarioMIP ssp119. Earth System Grid Federation. <https://doi.org/10.22033/ESGF/CMIP6.11045>.
76. Li L, Yu Y, Tang Y, Lin P, Xie J, Song M, et al. 2020. The Flexible Global Ocean-Atmosphere-Land System Model Grid-Point Version 3 (FGOALS-g3): description and evaluation. *J Adv Model Earth Syst* 12(9):e2019MS002012, <https://doi.org/10.1029/2019MS002012>.
77. Li L. 2019. CAS FGOALS-g3 model output prepared for CMIP6 CMIP historical. Earth System Grid Federation. <https://doi.org/10.22033/ESGF/CMIP6.3356>.
78. Li L. 2019. CAS FGOALS-g3 model output prepared for CMIP6 ScenarioMIP ssp119. Earth System Grid Federation. <https://doi.org/10.22033/ESGF/CMIP6.3462>.
79. Li L. 2019. CAS FGOALS-g3 model output prepared for CMIP6 ScenarioMIP ssp585. Earth System Grid Federation. <https://doi.org/10.22033/ESGF/CMIP6.3503>.
80. Döscher R, Acosta M, Alessandri A, Anthoni P, Arsouze T, Bergman T, et al. 2022. The EC-Earth3 Earth system model for the Coupled Model Intercomparison Project 6. *Geosci Model Dev* 15(7):2973–3020, <https://doi.org/10.5194/gmd-15-2973-2022>.
81. EC-Earth (EC-Earth Consortium). 2020. EC-Earth-Consortium EC-Earth3-Veg-LR model output prepared for CMIP6 CMIP historical. Earth System Grid Federation. <https://doi.org/10.22033/ESGF/CMIP6.4707>.
82. EC-Earth. 2019. EC-Earth-Consortium EC-Earth3-Veg model output prepared for CMIP6 ScenarioMIP ssp585. Earth System Grid Federation. <https://doi.org/10.22033/ESGF/CMIP6.4914>.
83. EC-Earth. 2019. EC-Earth-Consortium EC-Earth3-Veg model output prepared for CMIP6 ScenarioMIP. Earth System Grid Federation. <https://doi.org/10.22033/ESGF/CMIP6.727>.
84. Jaakkola JJK. 2003. Case-crossover design in air pollution epidemiology. *Eur Respir J Suppl* 40:81s–85s, PMID: 12762580, <https://doi.org/10.1183/09031936.03.00402703>.
85. Tebaldi C, Arblaster JM. 2014. Pattern scaling: its strengths and limitations, and an update on the latest model simulations. *Clim Change* 122(3):459–471, <https://doi.org/10.1007/s10584-013-1032-9>.
86. Partanen AI, Leduc M, Matthews HD. 2017. Seasonal climate change patterns due to cumulative CO₂ emissions. *Environ Res Lett* 12(7):075002, <https://doi.org/10.1088/1748-9326/aa6eb0>.
87. Seneviratne SI, Donat MG, Pitman AJ, Knutti R, Wilby RL. 2016. Allowable CO₂ emissions based on regional and impact-related climate targets. *Nature* 529(7587):477–483, PMID: 26789252, <https://doi.org/10.1038/nature16542>.
88. Chavaillaz Y, Roy P, Partanen AI, Da Silva L, Bresson É, Mengis N, et al. 2019. Exposure to excessive heat and impacts on labour productivity linked to cumulative CO₂ emissions. *Sci Rep* 9(1):13711, PMID: 31548555, <https://doi.org/10.1038/s41598-019-50047-w>.
89. Hausfather Z, Marvel K, Schmidt GA, Nielsen-Gammon JW, Zelinka M. 2022. Climate simulations: recognize the ‘hot model’ problem. *Nature* 605(7908):26–29, PMID: 35508771, <https://doi.org/10.1038/d41586-022-01192-2>.
90. Massoud EC, Lee HK, Terando A, Wehner M. 2023. Bayesian weighting of climate models based on climate sensitivity. *Commun Earth Environ* 4(1):365, <https://doi.org/10.1038/s43247-023-01009-8>.
91. Forster P, Storelvmo T, Armour K, Collins W, Dufresne JL, Frame D, et al. 2021. The earth’s energy budget, climate feedbacks, and climate sensitivity. In: *Climate Change: The Physical Science Basis. Contribution of Working Group I to the Sixth Assessment Report of the Intergovernmental Panel on Climate Change*. Masson-Delmotte V, Zhai P, Pirani A, Connors SL, Péan C, Berger S, et al., eds. Cambridge, UK: Cambridge University Press, 923–1054.
92. OSF (Official Statistics of Finland). 2022. Population structure. <https://stat.fi/en/statistics/vaerak> [accessed 23 January 2022].
93. OSF. 2022. Population projection. <https://stat.fi/en/statistics/vaenn> [accessed 23 January 2022].
94. OSF. 2022. Causes of death. <https://stat.fi/en/statistics/ksyyt> [accessed 23 January 2022].
95. Mähönen M, Salomaa V, Torppa J, Miettinen H, Pyörälä K, Immonen-Räihä P, et al. 1999. The validity of the routine mortality statistics on coronary heart disease in Finland: comparison with the FINMONICA MI register data for the years 1983–1992. Finnish multinational MONitoring of trends and determinants in Cardiovascular disease. *J Clin Epidemiol* 52(2):157–166, PMID: 10201658, [https://doi.org/10.1016/s0895-4356\(98\)00145-0](https://doi.org/10.1016/s0895-4356(98)00145-0).
96. Basu R. 2009. High ambient temperature and mortality: a review of epidemiologic studies from 2001 to 2008. *Environ Health* 8:40, PMID: 19758453, <https://doi.org/10.1186/1476-069X-8-40>.
97. Åström DO, Forsberg B, Rocklöv J. 2011. Heat wave impact on morbidity and mortality in the elderly population: a review of recent studies. *Maturitas* 69(2):99–105, PMID: 21477954, <https://doi.org/10.1016/j.maturitas.2011.03.008>.
98. van Steen Y, Ntarladima AM, Grobbee R, Karssen D, Vaartjes I. 2019. Sex differences in mortality after heat waves: are elderly women at higher risk? *Int Arch Occup Environ Health* 92(1):37–48, PMID: 30293089, <https://doi.org/10.1007/s00420-018-1360-1>.
99. Achebak H, Devolder D, Ballester J. 2019. Trends in temperature-related age-specific and sex-specific mortality from cardiovascular diseases in Spain: a national time-series analysis. *Lancet Planet Health* 3(7):e297–e306, PMID: 31230996, [https://doi.org/10.1016/S2542-5196\(19\)30090-7](https://doi.org/10.1016/S2542-5196(19)30090-7).
100. Murage P, Kovats S, Sarran C, Taylor J, McInnes R, Hajat S. 2020. What individual and neighbourhood-level factors increase the risk of heat-related mortality? A case-crossover study of over 185,000 deaths in London using high-resolution climate datasets. *Environ Int* 134:105292, PMID: 31726356, <https://doi.org/10.1016/j.envint.2019.105292>.
101. Sera F, Armstrong B, Tobias A, Vicedo-Cabrera AM, Åström C, Bell ML, et al. 2019. How urban characteristics affect vulnerability to heat and cold: a multi-country analysis. *Int J Epidemiol* 48(4):1101–1112, PMID: 30815699, <https://doi.org/10.1093/ije/dy2008>.
102. Kovats RS, Hajat S. 2008. Heat stress and public health: a critical review. *Annu Rev Public Health* 29:41–55, PMID: 18031221, <https://doi.org/10.1146/annurev.publhealth.29.020907.090843>.
103. Bouchama A, Dehbi M, Mohamed G, Matthies F, Shoukri M, Menne B. 2007. Prognostic factors in heat wave related deaths: a meta-analysis. *Arch Intern Med* 167(20):2170–2176, PMID: 17698676, <https://doi.org/10.1001/archinte.167.20.ira70009>.
104. Semenza JC, Rubin CH, Falter KH, Selanikio JD, Flanders WD, Howe HL, et al. 1996. Heat-related deaths during the July 1995 heat wave in Chicago. *N Engl J Med* 335(2):84–90, PMID: 8649494, <https://doi.org/10.1056/NEJM199607113350203>.

105. McMichael AJ, Woodruff RE, Hales S. 2006. Climate change and human health: present and future risks. *Lancet* 367(9513):859–869, PMID: [16530580](https://doi.org/10.1016/S0140-6736(06)68079-3), [https://doi.org/10.1016/S0140-6736\(06\)68079-3](https://doi.org/10.1016/S0140-6736(06)68079-3).
106. Wallace RF, Kriebel D, Punnett L, Wegman DH, Amoroso PJ. 2007. Prior heat illness hospitalization and risk of early death. *Environ Res* 104(2):290–295, PMID: [17306249](https://doi.org/10.1016/j.envres.2007.01.003), <https://doi.org/10.1016/j.envres.2007.01.003>.
107. Kalkstein LS, Greene JS. 1997. An evaluation of climate/mortality relationships in large U.S. cities and the possible impacts of a climate change. *Environ Health Perspect* 105(1):84–93, PMID: [9074886](https://doi.org/10.1289/ehp.9710584), <https://doi.org/10.1289/ehp.9710584>.
108. Keatinge WR, Donaldson GC, Cordioli E, Martinelli M, Kunst AE, Mackenbach JP, et al. 2000. Heat related mortality in warm and cold regions of Europe: observational study. *BMJ* 321(7262):670–673, PMID: [10987770](https://doi.org/10.1136/bmj.321.7262.670), <https://doi.org/10.1136/bmj.321.7262.670>.
109. Baccini M, Kosatsky T, Analitis A, Anderson HR, D'Ovidio M, Menne B, et al. 2011. Impact of heat on mortality in 15 European cities: attributable deaths under different weather scenarios. *J Epidemiol Community Health* 65(1):64–70, PMID: [19858539](https://doi.org/10.1136/jech.2008.085639), <https://doi.org/10.1136/jech.2008.085639>.
110. Heaviside C, Vardoulakis S, Cai XM. 2016. Attribution of mortality to the urban heat island during heatwaves in the West Midlands, UK. *Environ Health* 15(suppl 1):S27, PMID: [26961286](https://doi.org/10.1186/s12940-016-0100-9), <https://doi.org/10.1186/s12940-016-0100-9>.
111. Chapman S, Watson JEM, Salazar A, Thatcher M, McAlpine CA. 2017. The impact of urbanization and climate change on urban temperatures: a systematic review. *Landsc Ecol* 32(10):1921–1935, <https://doi.org/10.1007/s10980-017-0561-4>.
112. Deilami K, Kamruzzaman M, Liu Y. 2018. Urban heat island effect: a systematic review of spatio-temporal factors, data, methods, and mitigation measures. *Int J Appl Earth Obs Geoinf* 67:30–42, <https://doi.org/10.1016/j.jag.2017.12.009>.
113. Hondula DM, Georgescu M, Balling RC Jr. 2014. Challenges associated with projecting urbanization-induced heat-related mortality. *Sci Total Environ* 490:538–544, PMID: [24880543](https://doi.org/10.1016/j.scitotenv.2014.04.130), <https://doi.org/10.1016/j.scitotenv.2014.04.130>.
114. Lay CR, Sarofim MC, Vodonos Zilberg A, Mills DM, Jones RW, Schwartz J, et al. 2021. City-level vulnerability to temperature-related mortality in the USA and future projections: a geographically clustered meta-regression. *Lancet Planet Health* 5(6):e338–e346, PMID: [34022145](https://doi.org/10.1016/S2542-5196(21)00058-9), [https://doi.org/10.1016/S2542-5196\(21\)00058-9](https://doi.org/10.1016/S2542-5196(21)00058-9).
115. Krayenhoff ES, Moustaoui M, Broadbent AM, Gupta V, Georgescu M. 2018. Diurnal interaction between urban expansion, climate change and adaptation in US cities. *Nat Clim Chang* 8(12):1097–1103, <https://doi.org/10.1038/s41558-018-0320-9>.
116. Broadbent AM, Krayenhoff ES, Georgescu M. 2020. The motley drivers of heat and cold exposure in 21st century US cities. *Proc Natl Acad Sci USA* 117(35):21108–21117, PMID: [32817528](https://doi.org/10.1073/pnas.2005492117), <https://doi.org/10.1073/pnas.2005492117>.
117. Colston JM, Zaitchik BF, Badr HS, Burnett E, Ali SA, Rayamajhi A, et al. 2022. Associations between eight Earth observation-derived climate variables and enteropathogen infection: an independent participant data meta-analysis of surveillance studies with broad spectrum nucleic acid diagnostics. *Geohealth* 6(1):e2021GH000452, PMID: [35024531](https://doi.org/10.1029/2021GH000452), <https://doi.org/10.1029/2021GH000452>.
118. Borge R, Requía VJ, Yagüe C, Jhun I, Koutrakis P. 2019. Impact of weather changes on air quality and related mortality in Spain over a 25 year period [1993–2017]. *Environ Int* 133(pt B):105272, PMID: [31675571](https://doi.org/10.1016/j.envint.2019.105272), <https://doi.org/10.1016/j.envint.2019.105272>.
119. Ruosteenoja K, Jylhä K. 2021. Projected climate change in Finland during the 21st century calculated from CMIP6 model simulations. *Geophysica* 56(1):39–69.
120. Romanello M, McGushin A, Di Napoli C, Drummond P, Hughes N, Jamart L, et al. 2021. The 2021 report of the *Lancet* Countdown on health and climate change: code red for a healthy future. *Lancet* 398(10311):1619–1662, PMID: [34687662](https://doi.org/10.1016/S0140-6736(21)01787-6), [https://doi.org/10.1016/S0140-6736\(21\)01787-6](https://doi.org/10.1016/S0140-6736(21)01787-6).
121. Tobias A, Hashizume M, Honda Y, Sera F, Ng CFS, Kim Y, et al. 2021. Geographical variations of the minimum mortality temperature at a global scale: a multicountry study. *Environ Epidemiol* 5(5):e169, PMID: [34934890](https://doi.org/10.1097/EE9.000000000000169), <https://doi.org/10.1097/EE9.000000000000169>.